

Modeling and simulation of concrete carbonation in 1-d using two-point flux approximation

Master's thesis in Applied and Computational Mathematics

Tineke Røe



Department of Mathematics
University of Bergen

November 20, 2013

To my father and brothers

Acknowledgement

I would like to thank Florin Radu and Inga Berre for being my supervisors on this master's thesis, and for their help and support. I also would like to thank Kristine Lysnes for guidance in more general matters during my period of study.

In December 2012, I was able to stay in two weeks at Eindhoven University of Technology in the Netherlands thanks to the NUPUS collaboration between the University of Bergen, TU Delft, TU Eindhoven, University of Stuttgart, Utrecht University and Wageningen University. Sorin Pop and Adrian Muntean were most kind to me during my stay there.

I will thank my friends here in Bergen and all the friendly people I have gotten to know here. A special thanks to all the nice people down at the "old" Department of Mathematics.

Bergen November 2013.

Abstract

In this master's thesis we will model concrete carbonation using mass conservation equations and Darcy's law. We then get a set of coupled partial differential equations. We also have a ordinary differential equation modeling porosity change. These equations are discretized using two-point flux approximation for 1-d in space, and Euler implicit in time. We have a non-linear pressure equation which is linearized using Newton method. We run simulations, and the results are compared to a constructed analytical solution and to examples in the literature.

Contents

Abstract	v
Symbols	ix
Introduction	1
1 Concrete carbonation	5
1.1 Reinforced concrete	5
1.1.1 Historical perspective	5
1.1.2 The ingredients of concrete	6
1.1.3 Reinforcement	8
1.2 Concrete carbonation	9
1.2.1 Hydration	9
1.2.2 The process of concrete carbonation	10
1.2.3 The influence of humidity	11
1.2.4 Carbonation depth	12
1.2.5 The effects of carbonation	13
1.2.6 Modeling concrete carbonation	13
2 Mathematical model	15
2.1 Flow in porous media	15
2.1.1 Porous media properties	15
2.1.2 Mass conservation	17
2.1.3 Darcy's law	19
2.1.4 Diffusion and transport equations	20
2.2 Chemical reactions	21
2.2.1 Reaction rate	21
2.2.2 Dissolution/Precipitation	22
2.3 The model	23
2.3.1 The water flux equations	24
2.3.2 The equations of the chemical species	25

2.3.3	The equation for the porosity	26
2.3.4	Simplifications	27
2.3.5	Numerical solution approach	28
3	Numerical modeling	31
3.1	Grid	31
3.2	Spatial discretization	33
3.2.1	Finite difference approximation	33
3.2.2	Control volume methods	34
3.2.3	Boundary conditions	37
3.2.4	Diffusion-advection equation	42
3.3	Temporal discretization	45
3.4	Nonlinear equations	46
3.5	Coupling the equations	49
3.6	Discretization of the set of equations	51
4	Numerical results	55
4.1	Comparison with analytical solution	55
4.1.1	The set of equations	55
4.1.2	Comparison results	58
4.2	Numerical simulations	61
5	Conclusion	67
	References	69

Symbols

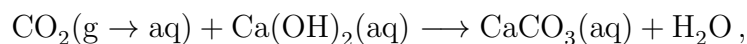
A	concentration of $\text{CO}_2(\text{aq})$, carbon dioxide, liquid
a	concentration of $\text{CO}_2(\text{g})$, carbon dioxide, gas
B	concentration of $\text{Ca}(\text{OH})_2(\text{aq})$, calcium hydroxide, liquid
b	concentration of $\text{Ca}(\text{OH})_2(\text{s})$, calcium hydroxide, solid
C	concentration of $\text{CaCO}_3(\text{aq})$, calcium carbonate, liquid
c	concentration of $\text{CaCO}_3(\text{s})$, calcium carbonate, solid
D_A	diffusion coefficient for CO_2 in water
D_a	diffusion coefficient for CO_2 in air
D_B	diffusion coefficient for $\text{Ca}(\text{OH})_2$ in water
D_C	diffusion coefficient for CaCO_3 in water
f_{Diss}	production rate by dissolution
f_{Prec}	production rate by precipitation
f_x	partial derivative of f with respect to x
f_t	partial derivative of f with respect to t
H	Henry constant
h	length of space step
i	index space
j	index time
k	relative permeability
K_S	absolute permeability
K	effective permeability
L	liter
m	molecular weight
p	atmospheric pressure
p_c	capillary pressure
\mathbf{q}	water flux
q	water flux, 1-dimension
r	rate constant
s	switcher for variable of not variable porosity
S_{Diss}	dissolution constant
S_{Prec}	precipitation constant

t	time variable
x	space variable
Z_ϕ	regularization parameter
α	parameter in van Genuchten-Mulean parameterization
γ	reaction rate
δ	regularization parameter
ρ	density
σ	stoichiometric coefficient
τ	length time-step
ϕ	porosity
ϕ_w	water saturation (water fraction)
$\phi_{w,max}$	maximal water saturation
ϕ_g	gas saturation (gas fraction)
Ω	total volume
Ω_p	pore volume
Ω_s	matrix volume

Introduction

Concrete has widely been used as a building material since Portland cement was invented in the 19th century [23]. Its popularity comes from the facts that it is easy to produce and simple to get hold on [35]. That makes it fairly cheap. Due to its plasticity it can be easily formed, and is used for building, bridges, roads and other constructions. Combined with steel reinforcement, concrete form a composite building material with both compressive strength, due to the concrete, and tensile strength, from the steel. Reinforced concrete can therefore hold heavier loads and give rise to more slender constructions. Its fire residence also plays an important role in its popularity.

The strength and its durability is the most important properties of the concrete [35]. Both of safety and economical reasons we want the concrete structures to have a long service life. There are several things that can threaten the durability, strength and the life-time for a concrete structure [30]. One of the biggest threats for the durability of reinforced concrete structures, is concrete carbonation. Concrete is a porous material, having holes called pores inside with some water in them. Concrete carbonation is a chemical reaction in these pores, where the carbon dioxide from the air dissolves in the concrete's pore water and reacts with the dissolved lime from the concrete. The chemical reaction can be written as



that is, carbon dioxide goes from being a gas into water, inside the water it reacts with calcium hydroxide, and forms calcium carbonate and water [27].

Initially, the pore solution of concrete is alkaline because of the amount of dissolved lime, in the form of $\text{Ca}(\text{OH})_2$ in the pore water. This provides a natural protection of the steel reinforcement against corrosion. However, through the carbonation process the carbon dioxide are bonded with the lime, and the pore solution gets more and more acid. When the pH-value of the pore solution gets below 9, the protection of the reinforcement is weakened and corrosion can occur. The reaction moves like a reaction front with highly alkaline pore solution in front of the reaction front, and less

alkaline pore solution behind the reaction front. When doing laboratory experiments where concrete samples are exposed to CO_2 , this reaction front is shown where there is a rapid change in the pH-level.

When the reinforcement start to rust, two things happen. First, the cross section of the steel bars gets reduced, which weakens the reinforcements strength. On the other hand, the strength of the concrete can also get weakened as a result of the reinforcement corrosion. This due to the fact that when the reinforcement corrode, its volume will increase. Cracks will appear in the concrete as a result of this expansion. These cracks runs alongside the reinforcement, and the concretes resistance against stresses decreases [32]. If not discovered and taken care of, the reduction in strength of concrete constructions can result in big material damages and in the worst case, in the lost of human lives. In [43] they give several examples on concrete structures like bridges and buildings, which collapsed because of corrosion and of cracking.

Concrete carbonation is a chemical reaction happening in concrete which can be modeled by using mass conservation laws, providing us with differential equation we can solve using standard numerical solving techniques. What is the primary interest for modeling concrete carbonation, is to study how the reaction front moves towards the reinforcement. In building engineering they want to know this, to be able to predict the service life of a concrete structure, that is, how long its strength will be maintained. When it starts cracking, repairs has to be down, to avoid collapses, and they want to know when they need to start checking for example a building for cracks. They want to explore different different kinds of concrete, to see which kind provides the best of steel reinforcement against corrosion. Ordinary Portland cement is the primary used kind of cement to make concrete, but due to the high CO_2 emission when it is produced, other cement types are used more and more.

Modeling concrete carbonation is not only of interest for building engineers. It can also be regarded as a chemical problem, studying and modeling the chemical reactions that happen inside the concrete, and as a mathematical problem, analyzing the equations and the model itself. Papadakis et al. [32, 33] study the reaction from a chemical perspective, looking at the all the different species and reaction inside the concrete, while Saetta et al, [41] and Steffens et al. [44, 45] look at the problem from a engineering point of view. Meier et al. [27], Peter et al. [36] and Muntean et al. [28, 29] follow the path of Papadakis et al., but in a more mathematical direction.

We will base our studies on the work of Radu et al. [39]. They follow the path of Papadakis et al. further, but attempts to combine the mass conservation equations of the chemical species involved in the reaction, with

flow equations used in reservoir modeling. Whereas the other models are 1-d space models, Radu et al. set up the model in two space dimensions. We will only consider one space dimensional like in the other models. Radu et al. also adds an equation for variable porosity to the model.

We will set up the mass conservation equations for CO_2 , Ca(OH)_2 and Ca(OH)_2 in the water phase, the mass conservation equations for water and the water flux equation from Darcys law. These form a coupled set of partial differential equations. In addition we will have a ordinary differential equation modeling the change in the porosity due to the dissolution of Ca(OH)_2 from the solid concrete into the pore water, and the forming of solid CaCO_3 as a result of the concrete carbonation reaction. The former will increase the porosity, while the latter will decrease the porosity of the concrete.

This set of equations will be solved using two-point flux approximation in space and Euler implicit in time. The results of the simulations will be compared to results in Radu et al. [39], Meier et al. [27] and Peter et al. [36].

Chapter 1 will be about reinforced concrete and concrete carbonation, giving some backgrounds knowledge to understand the reaction we are going to model, and to realize why studying concrete carbonation is of importance.

In chapter 2, the mathematical model will be derived from mass conservation and porous media flow.

Then chapter 3 deals with the discretization of equations, and we account for how we will solve the set of equations numerically.

In chapter 4, the results from the numerical simulations are given.

Chapter 5 give some conclusions and further discussions.

Chapter 1

Concrete carbonation

This chapter will give some background for concrete carbonation, the process we want to model. First there will be some general background about reinforced concrete, the historical background and why it is used. Then there will be some general about concrete and about reinforcement. After that we will look at the at the reaction from a chemical point of view. The background is chemistry and building engineering.

1.1 Reinforced concrete

Concrete is the finished material you get when adding cement and water. It is used for architectural constructions, pavements, bridges, roads, parking structures, dams, reservoirs, pipes and fences. It is widely used because it is simple to produce and easy to get hold of [35].

1.1.1 Historical perspective

During the Roman Empire, 1st century BC to 5th century AD, they developed the technique of building with concrete, and used it for water pipes, aqueducts, buildings and bridges. The use of concrete enabled them to make arches and vaults, often combined with bricks and stones for strength [12]. A well known example of one of their buildings, is the Pantheon still standing in Rome. It was build around AD 120 and is famous for its big concrete dome [20].

The knowledge of concrete seems to have been lost with the fall of the Roman empire, and not taken up again before in the 18th century [35]. Throughout the 19th several people developed the technique further, ending up with a stronger concrete. And also laid the theoretical foundation for

the use of concrete. They also found out that by combining the other new building material iron and steel with concrete, men got a building material which both had good compressive and tensile strength. This combination is called reinforced concrete, and from the beginning of the 20th century it was spread around the world by education and research [33]. This enable them to build less compact concrete buildings, with open space underneath the building or and big windows like in Le Corbusier's Villa Savoye completed in 1931.

The strength and its durability is the most important properties of the concrete [35], and have been the subject of the development and studies about concrete. In the later years, with the focus on reducing the CO₂ emission, new ways of making concrete are sought. The production of ordinary Portland cement (OPC) which originally has been the main component of concrete, releases a lot of CO₂. Concrete is much used, and because this and because almost as much CO₂ is released in the production as as much cement are produced, the cement industry actually is responsibly for about 5% of the global emission of CO₂ [42]. One way to reduce the emission of carbon dioxide, is to use less cement in the concrete, and other is to absorb CO₂ back into the concrete by means of carbonation [6,42].

1.1.2 The ingredients of concrete

The concrete the Romans the applied, was a mixture of sand, lime and water together with aggregates like broken stones (rubble) and volcanic dust [12, 25, 35]. The main difference between the concrete in ancient times and the modern one, is the use of cement in making of the concrete. The modern concrete is made of water, cement, aggregates, additives and admixes [35].

Cement was discovered in the 19th century [12]. To make cement for example earth and stones are fired and being ground into a powder. This powder can be mixed with water, and becomes hard when it dries. Consequently cement is called the binder. As in ancient times, aggregates are added to make the concrete stronger. Typically, they are gravel of different sizes. Even though the aggregates mostly are of natural material, artificial material like clay or foamed glass, made of recycled glass, are also being used. Applying foamed glass to the concrete, makes it lighter.

Portland cement is used in most types of concrete, and was originally the main component. However, emission of carbon dioxide is a side-effect cement production. As much as 1 ton of CO₂ is released into the atmosphere for every ton of cement produced [42]. To reduce the carbon dioxide emission in the production of concrete, other mineral components are added. These are for example blast-furnace slag, limestone dust, pulverized fuel ash (PFA) or

burnt shale. Fuel ash, also called fly ash, is produced from burning charcoal, and is the most used additive. It has similar properties to cement in the way it has a hydraulic effect, it gets hard when mixed with water and dries, and thus contributes to the strength of cement. Therefore it is a good substitute for Portland cement in concrete production, but there are limits on the amount that can be added, because when too much is used, fly ashes can reduce the durability of the concrete [35]. Another frequently used additive is silica fume which is a by-product of silicon production. It is also a gray powder like cement and fly ashes [19]. Other additives can be for example pigments or rock dust added to change the look of the surface.

The relationship between the chemical components of cement varies for the different kind of cements, but the main components are usual calcium oxide CaO , and silicon dioxide SiO_2 . In Portland cement the main component is calcium oxide, almost 65 % of the total amount of cement, and silicon dioxide about 20 % [19, 44]. Table 1.1 compares Portland cement with silica fume and two sorts of fly ash [19].

The admixes usually don't influence the hard concrete, but it helps the wet concrete to be more fluent and easier to work with. To improve the frost resistance of the concrete, air bubbles are intentionally added, creating spherical air pockets in the hard concrete.

Table 1.1: Chemical components of different kinds of cement.

Chemical	Formula	Portland Cement	Class F Fly Ash	Class C Fly Ash	Silica Fume
Calcium oxide	CaO	62 %	5 %	21 %	< 1 %
Silicon dioxide	SiO_2	21 %	52 %	35 %	85 – 97 %
Aluminum oxide	Al_2O_3	5 %	23 %	18 %	
Iron(III) oxide	Fe_2O_3	3 %	11 %	6 %	

The strength, durability and other properties of the concrete, like porosity, depends on the water/cement (w/c) ratio, the kind of aggregates and additives used and the quantities of those. The different types of concrete are covered by international and national standards. All the stresses which a concrete structure will be exposed to, has to be calculated thoroughly, making sure that the structure can stand all the stresses and the pressure. When the concrete by itself is not strong enough, some kind of reinforcement has to be added to the concrete.

When planning of concrete buildings, the interior climate has to be taken into account. The effects to be considered, are for example the influence of outside temperature and moisture on the interior climate, and the movement of the interior air. Another concern to take into account, is temperature regulation and energy saving. It shouldn't get too hot inside the building in the summer, or too cold in the winter. The outside walls of the concrete building should also be impregnated, to avoid water and moisture getting in [23].

We will in this thesis consider ordinary Portland concrete (OPC) which used to be the primarily type of concrete, and much research is done on concrete carbonation and the effect on reinforcement for Portland concrete.

1.1.3 Reinforcement

A concrete building will typically be subjected to tensile and compressive tension, the tensile tension stretching the material, and the compressive tension pressing it together. Concrete has naturally high degree of compressible strength, while its tensile strength is 10% of its compressive strength [1, 35]. Therefore if a concrete structure is going to be exposed to tensile forces, it needs to be strengthened with reinforcement, otherwise it will break.

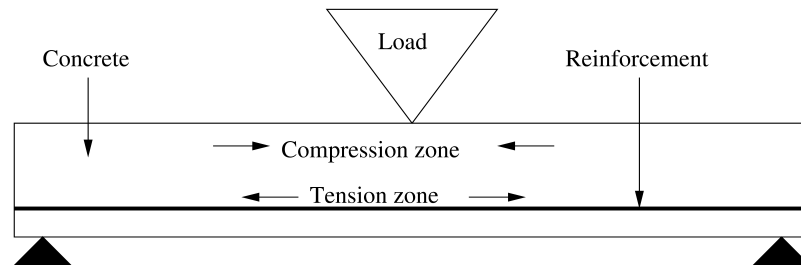


Figure 1.1: Reinforced concrete with compressive and tensile forces.

Figure 1.1 shows a beam supported at the ends and loaded in the middle. This causes bending stresses, with compression stress on the top of the beam, and tensile stresses in the bottom. The compression presses the concrete together, and the tension in the bottom tries to pull it apart. With a heavy load and no reinforcement, the beam will in this case break in the bottom. A reinforcement near the bottom of the beam, prevents the beam from breaking. If the beam on the other hand was supported in the middle and loaded in the ends, it would be subjected to tension on the top and compression in the bottom. Then the reinforcement had to be added near the top of the beam [1]. Thus it is important where you place the reinforcement.

Steel is the most common used material to reinforce concrete, but there are also reinforcements made of natural or synthetic fibers [1]. It is not only important what kind of reinforcement you use and where you place it, you also have to be sure the enough reinforcements to withstand the forces. Because of its high tensile resistance, the amount of steel needed is relative small, and this makes it well fitted as a reinforcement. Another reason for steel to be well suited, is the way concrete and steel act together. When concrete dries, it bonds to steel. As a result, stresses are transfered effectively between the steel reinforcement and concrete. Concrete and steel also respond similarly to temperature changes, such that the good bond is kept between them.

In addition to withstand tensile forces, reinforcement is used to resist shear stresses and also compressible stresses. Concrete has a high degree of compressive strength, but steel has an even higher degree of compressive strength, as much as 20% [1]. Therefore, steel is used in columns to reduce their diameters.

The concrete cover of the reinforcement have to be of the right thickness. It has to be thick enough to protect the reinforcement against corrosion and to ensure the ends of the reinforcement are fasten properly. On the other hand, if the concrete cover is too thick, there can be areas where the tensile forces will make the concrete break.

1.2 Concrete carbonation

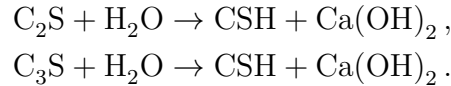
The strength and its durability is the most important properties of the concrete [35]. There are several things that can threaten these properties and the life-time for a concrete structure. For reinforced concrete the most severe of these are corrosion of the reinforcement by concrete carbonation or by chlorides. The latter is mostly attacks by see-water or salts used for melting ice on roads. Concrete can also be object of corrosion, then from frost attacks, attack of chemicals or abrasion, if the concrete gets worn out. For buildings on land, it is frost attacks and carbonation of concrete that can weaken their durability.

1.2.1 Hydration

When mixed with water, there is a chemical reaction resulting in the cement getting hard. The cement bonds the water, and this bonding is called hydration. The bonded water can not evaporate, and the amount of bonded water gives the water/cement ratio. When for example the total amount of

bonded water is about 40 %, then w/c is 0.40 [23]. The hydration process is fast in the beginning, and gradually slows down. It stops when there is no water left.

The primarily components of Portland cement are calcium oxide CaO, and silicon dioxide SiO₂, see table 1.1. We will here give the main hydration reactions. They can be given as



We have here used the notation from Papadakis et al. [33] and Peter et al. [36]. C₂S stands for 2 CaO · SiO₂ (dicalcium silicate) and C₃S is 3 CaO · SiO₃ (tricalcium silicate). C₂S and C₃S reacts with the water H₂O when cement is mixed with water. The products of the reactions are Ca(OH)₂ (calcium hydroxide) and CSH (calcium silicate hydrate). CSH stands for 3 CaO₂ · 2 SiO₂ · 3 H₂O, and is the main source of strength of concrete [33].

It is usually taken into care to keep the pores filled with water the first days. Then the hydration reactions can continue. This is called curing [30, 33].

1.2.2 The process of concrete carbonation

Concrete is of some degree a porous media, that is, it has small holes inside. These can be isolated or connected to the border of the concrete. We are interested in those with connection to the outside of the concrete. These pores are filled with air and/or humidity, see fig. 1.2. The carbon dioxide in the air flow through the pores, dissolve into the water in the pores and react with the hydration products Ca(OH)₂ and CSH. Also non-hydrated elements C₂S and C₃S will carbonate, that is, react with the CO₂. The main products of these reactions are CaCO₃ and 3CaCO₃ · 2SiO₂ · 3H₂O from the carbonation of Ca(OH)₂ and CSH respectively. These carbonation processes cause a decrease in the porosity of the concrete. This decrease can be measured [33]. The decrease in porosity has a good effect on the concrete, making it stronger. Carbonation takes CO₂ and bind it in the concrete. This is stated to be have been used to produce a more environmentally friendly concrete [6].

When it comes to reinforced concrete, there is another result of the carbonation which has a weakening effect on the concrete construction. The reinforcement is naturally protected inside the concrete because of the high amount of lime in form of Ca(OH)₂. Ca(OH)₂ get dissolved from the solid concrete into the pore water, and it makes the pore water alkaline. This

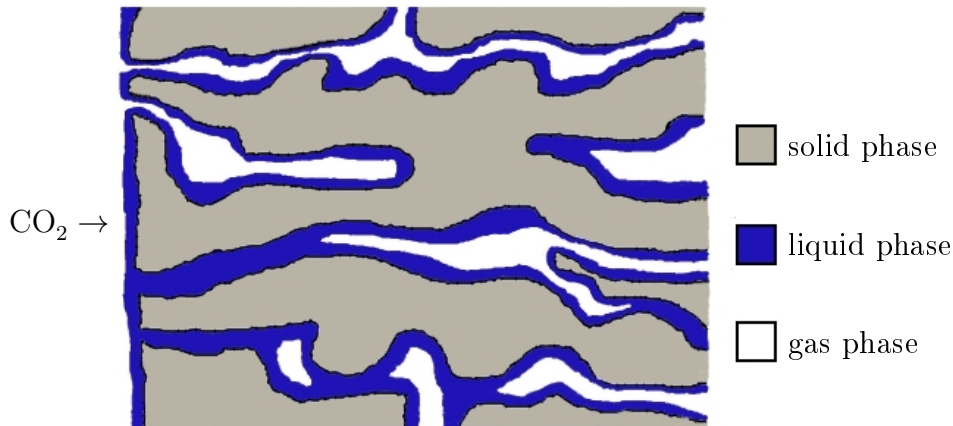
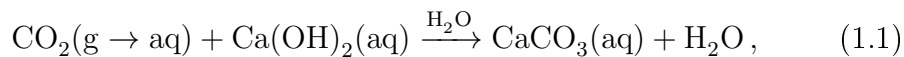


Figure 1.2: CO_2 in the air diffuses in to the concrete pores.

alkaline solution protects the steel from corrosion forming and maintaining a thin oxide layer around the reinforced bars [32]. But carbonation of $\text{Ca}(\text{OH})_2$ makes the pore water more and more acid. The reaction we then are interested in to model is the following



where the subscription “g” and “aq” refers to the gas and liquid forms. In words, carbon dioxide comes into the concrete through the air and get dissolved into the pore water. In the water, CO_2 reacts with the dissolved calcium hydroxide. The products of this reaction are calcium carbonate and water.

The same is not the case for CSH or C–S–H. It does not affect the alkalinity of the pore solution. C–S–H doesn’t dissolve into the pore water either [45]. They state that this is the main reaction. It’s not the formation of CaCO_3 which makes the pore water more acid, it is the bonding of $\text{Ca}(\text{OH})_2$ in the solid CaCO_3 - reducing it from the pore water, which makes it more acid.

1.2.3 The influence of humidity

Because the concrete carbonation reaction happens in water, no humidity inside in the concrete pore space, will result in no concrete carbonation. On the other hand, water filled pores will block the flow of carbon dioxide. Figure 1.2 show a pore system filled with water and air. When the pores

are completely filled with water near the concrete wall, the CO_2 flow will be blocked.

In [30] it is concluded that the humidity is the most important factor when determining the rate of carbonation, and to get a good description of the carbonation process, it is necessary to include the moisture variations inside the concrete due to the humidity changes on the surface of the concrete.

1.2.4 Carbonation depth

During concrete carbonation, the pH-value inside the concrete changes. It can be thought of a layer moving forward, and men are interested in how fast this layer moves. This to be able to predict how long it takes before it reaches the reinforcement and leaving it without protection against corrosion. In the article of Villian et al. [49] they describe ways to measure carbonation depth [49], which is how far the reaction layer has reached into the concrete starting from the concrete wall.

The concrete carbonation reaction can be regarded as a moving-boundary problem because of the reaction being so fast compared to the diffusion [36]. In Muntean and Böhm [28] they look at the reaction as a moving-boundary problem, where the reaction front is the moving boundary.

The reaction of CO_2 is faster than it diffuses, and therefore we get a reaction front of a few millimeter that moves with the reaction through the concrete [45]. On the other side of the this reaction layer, have the $\text{Ca}(\text{OH})_2$ which reacts with CO_2 , decrease towards the front. In Meier et al. [27] they show that the decrease in $\text{Ca}(\text{OH})_2$ due to the reaction, is steeper than the decrease in CO_2 . The also show that the profiles for CO_2 in the air phases and CO_2 in the water phases, have the same profile when they are taken as dimensionless numbers.

There are several ways to define the reaction front or the carbonation depth. A easy way to give the reaction front or carbonation depth as proportional to the square root of time

$$s(t) = c_k \sqrt{t}. \quad (1.2)$$

They use this notation of the reaction front in Papadakis et al. [32]. The constant c_k varies given the type of concrete and the environment [30].

In Steffens et al. [45] the reaction front is given by the degree of carbonation $k = 0.9$. The degree of carbonation Steffens [44] defines as the dimensionless number for the amount of reacted CO_2 . The degree of carbonation can also be regarded as a measure on how much CaCO_3 is produced, and in Meier et al. [27] they define the reaction front as where the dimensionless variable for CaCO_3 is equal to 0.9. The reaction front can also be

given as by the amount of Ca(OH)_2 , which is done in Peter et al. [36]. For the dimensionless numbers, the amount of Ca(OH)_2 is $1 - k$, which gives the carbonation front where the Ca(OH)_2 amount is equal to 0.1. Because the decrease in Ca(OH)_2 is steeper than the decrease in CO_2 , the Ca(OH)_2 can give a clearer indicator for the reaction front than the CO_2 profile. The reason for the profile of CO_2 to be less steep, is because it has to move to the reaction zone [36].

In Muntean and Böhm [28] and Muntean et al. [29] they give a formula for the speed of the reaction layer.

1.2.5 The effects of carbonation

The reinforcements protection get damaged through the carbonation, and with this protection away, the reinforcement can be a subject of corrosion. Corrosion of steel forms hydrated iron oxide, rust. It can only happen when there is both water and oxygen present [13]. Thus, corrosion will not automatically happen when the pore solution has gotten acid. The corrosion both reduces the diameter of the reinforcement's cross-section, reducing its strength, and giving rise to cracking of the concrete cover. The last as a result of the volume increase due to the corrosion, because the products of the corrosion take up more space than the originally metal [30, 33]. See chapter 9 [30] for pictures of corroded reinforcement and more details about reinforcement corrosion.

1.2.6 Modeling concrete carbonation

Papadakis et al. [32] gives a model given much of the chemical processes giving the reaction of the carbonation. By laboratory experiments they show that the porosity and the size of the pores of Ordinary Portland Cement goes down with carbonation. They then state that the effect of water is more important than the change in porosity, because the pore volume filled with air, is the volume carbon dioxide can diffuse through. In their article, they also consider the hydration process which results in formation of calcium hydroxide, Ca(OH)_2 , from the reaction of the main components of Portland cement [44], calcium oxide CaO and silicon dioxide SiO_2 , with water H_2O . The other product of this reaction, next to Ca(OH)_2 , is calcium silicate hydrate CSH. CSH will also react with CO_2 , just like Ca(OH)_2 , as well as some other combinations of CaO and SiO_2 will, C_2S and C_3S . They give an equation for the change in porosity, and they look at the propagation speed of the reaction layer.

There are two ways the humidity inside the pores can increase, by concrete carbonation, and by water or humidity entering from outside of the concrete. The latter given by the weather conditions. The humidity of the concrete is effected by its environment. Concrete buildings situated in places with a dry climate, will contain less humidity or water, than buildings situated in wet places. Both very dry and very wet environments reduce the concrete carbonation process. One approach to the concrete carbonation problem, is to look at the influence of the humidity of the outside environment on the concrete carbonation reaction and how the reaction layer propagates. In [45] and [44] they look at the seasonly change relative pore humidity compared to the carbonation degree, and find some correlation between the relative humidity and degree of carbonation. In wet seasons they find that the carbonation degree is less steep than in dry seasons, see [45]. Their results are compared with results from tests done under laboratory conditions by Thomas and Matthews [47]. Steffens et al. [45] follow the path of Saetta et al. [41], where they look closer to the influence of humidity and temperature on the reaction rates.

Peter et al. [36] use a similar complex model as Papadakis et al. [32] for the concrete carbonation reaction, involving the mass conservation equations for all the species involved in hydration and carbonation reactions in concrete. They conclude that CSH, C_2S and C_3S have little influence on the carbonation depth, and can be omitted from the model. And in Meier et al. [27] they do so, looking at the mass conservation equations of the species in the main concrete carbonation reaction, CO_2 , $Ca(OH)_2$ and $CaCO_3$ in the air and water phases. Both Peter et al. and Meier et al. consider the influence of humidity on the reaction, following the work of Steffens et al. and Saetta et al. [41,45].

In the work of Radu et al. [39], they continue this way. In addition they assume water flow inside the concrete, and look at variable porosity.

Chapter 2

Mathematical model

This chapter will provide the mathematical background for the model, and we will here set up the mathematical equations we will like to use to model concrete carbonation. The background is mass conservation. We will also use equations and theory from modeling in porous media, which is used for modeling the flow in for example an oil reservoir. Here the same equations will be sought to be used for modeling of the flow in concrete. We will use the same model as they did in the article of Radu et al. [39]. Thus what we wish to do in this chapter, is to explain the equations in their model.

2.1 Flow in porous media

The theory in this section is taken from [37]. Concrete is a porous medium, and we will here define the properties of porous media which we will consider in our model. The main equations for the flow in porous media, are equations of mass conservation, and Darcy's law.

2.1.1 Porous media properties

As already mentioned in section 1.2, concrete is a porous medium, which means it contains small holes called pores. The diameter of capillary pores are up to $1 \mu\text{m}$ [30], that is, they are in such a fine scale that we can not resolve them. We instead average over a scale which can be resolved. We choose a length scale where we can define meaningful averages over the pore scale and where experiments can be preformed in a laboratory. This length scale is denoted representative elementary volume (REV). This is typically on the order of one up to ten centimeters [31].

Let Ω denote this representative elementary volume. We will define the

porous media properties for this volume. If the material is assumed to be homogeneous, Ω can represent the total volume of the sample. We then denote the pore volume by Ω_p . This is the volume of all the pores in Ω . The solid part of the material is called matrix, and we denote the matrix volume Ω_s . The porosity is defined as the ratio between the pore volume Ω_p and the bulk volume Ω ,

$$\phi = \frac{\Omega_p}{\Omega}. \quad (2.1)$$

The porosity of concrete depends on the aggregates and the water to cement (w/c) ratio. Measurements can be done. In [21] a table of the porosity for different (w/c) values is given. From the definition of porosity we get the solid fraction

$$\phi_s = 1 - \phi. \quad (2.2)$$

In the pores of concrete, there are two phases, a water and a gas phase. Let Ω_w and Ω_g denote the volumes occupied with water and gas respectively. Then the water fraction or water saturation, is given by

$$\phi_w = \frac{\Omega_w}{\Omega_p}, \quad (2.3)$$

and the gas fraction by

$$\phi_g = \frac{\Omega_g}{\Omega_p}. \quad (2.4)$$

Further because the sum of the volume occupied with water and the volume occupied with gas is the pore volume

$$\Omega_w + \Omega_g = \Omega_p,$$

the sum of the water and the gas fraction equals one,

$$\phi_w + \phi_g = 1. \quad (2.5)$$

From this follows that the product of the porosity and the water saturation is the same as the amount of water divided by the total volume

$$\phi\phi_w = \frac{\Omega_p}{\Omega} \frac{\Omega_w}{\Omega_p} = \frac{\Omega_w}{\Omega}. \quad (2.6)$$

Thus $\phi\phi_w$ is a measure of the amount of water (or humidity) in Ω . Similarly, $\phi\phi_g$ gives the amount of gas in the volume Ω ,

$$\phi\phi_g = \frac{\Omega_g}{\Omega}. \quad (2.7)$$

Both products will depend on the water saturation, $\phi\phi_w$ directly, and $\phi\phi_g$ because the water and gas phases exclude each other. If we know the water fraction ϕ_w , we can find the gas fraction ϕ_g from eq. (2.5) and vice versa.

For our two phase problem, the capillary pressure p_c is the pressure difference over the water/air interface. We can express the capillary pressure as a function of the water saturation

$$p_c = p_c(\phi_w).$$

Or give the water saturation as a function of the capillary pressure

$$\phi_w = \phi_w(p_c). \quad (2.8)$$

2.1.2 Mass conservation

The main principle for modeling of flow and transport in porous media and in concrete, is the principle of mass conservation [30,37]. It comes from the conservation laws which gives that a physical quantity is preserved in a closed system [37]. That is, the change of mass inside a volume, has to be equal the amount of mass that is created inside the volume minus the mass that leaves the volume. We will derive the mass conservation equation in a similar way to what they do in [24] and in [2].

We start by giving an arbitrary volume Ω , with boundary $\partial\Omega$ and outer unit normal \mathbf{n} , see fig. 2.1. Inside this domain we can have water, air and

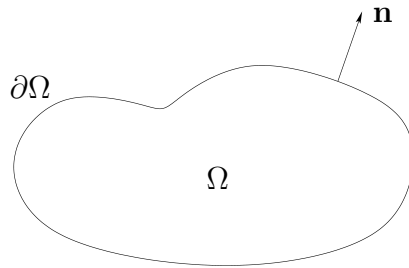


Figure 2.1: A domain Ω with boundary $\partial\Omega$ and outer unit normal \mathbf{n} .

several species. The volume density or the concentration of a species is given by its density ρ times the porosity ϕ . Then

$$\int_{\Omega} \phi\rho dV,$$

gives the mass inside Ω . And

$$\frac{\partial}{\partial t} \int_{\Omega} \phi \rho \, dV ,$$

gives the variation in the mass with respect to time. For this derivative not to be zero, we need either have a flux in or out of the domain Ω , or have a source or sink inside Ω . We will consider both a flux over the boundary and a source (or sink) term.

The net flux of the species over the boundary $\partial\Omega$ is given by

$$\int_{\partial\Omega} (\rho \mathbf{v}) \cdot \mathbf{n} \, dS ,$$

where \mathbf{n} is the outer unit normal on $\partial\Omega$, and \mathbf{v} denotes the volume flux density. When we let Q denote the inner source density, the total production (or destruction) is given by

$$\int_{\Omega} Q \, dV .$$

The mass conservation principle gives then

$$\frac{\partial}{\partial t} \int_{\Omega} \rho \, dV + \int_{\partial\Omega} (\rho \mathbf{v}) \cdot \mathbf{n} \, dS = \int_{\Omega} Q \, dV . \quad (2.9)$$

Equation (2.9) is the integral form of the mass conservation equation. From the divergence theorem [4]

$$\int_{\partial\Omega} (\rho \mathbf{v}) \cdot \mathbf{n} \, dS = \int_{\Omega} \nabla \cdot (\rho \mathbf{v}) \, dV ,$$

where $\nabla \cdot (\rho \mathbf{v})$ is the divergence of the flux density $\rho \mathbf{v}$. We also use differentiating through the integral, that is taking the derivative inside the integral [4], that is

$$\frac{\partial}{\partial t} \int_{\Omega} \phi \rho \, dV = \int_{\Omega} \frac{\partial}{\partial t} (\phi \rho) \, dV .$$

When we add the integrals together, we get the following equation

$$\int_{\Omega} \left(\frac{\partial}{\partial t} (\phi \rho) + \nabla \cdot (\rho \mathbf{v}) - Q \right) dV = 0 .$$

Because the domain Ω is arbitrary, this has to hold for all possible choices for Ω , and therefore the integrand has to vanish, and

$$\frac{\partial}{\partial t} (\phi \rho) + \nabla \cdot (\rho \mathbf{v}) = Q . \quad (2.10)$$

This is the general form of the mass conservation equation.

2.1.3 Darcy's law

We now want to find an expression for the water flow. We can not use the hydrodynamic flow equations, like the Navier-Stokes equation, to model the flow in the pores of the porous media. This because the friction between the flow and the walls of the pores is a dominating factor for flow in the pores [37]. Instead we use Darcy's law.

Darcy's law was originally derived by experiments of water flow through sand samples, measuring the velocity of the water, and the pressure on the top p_1 and the bottom p_2 of the sample. It was found that the velocity q of the water was proportional to the fraction between the pressure difference $\Delta p = p_1 - p_2$ and the height of the sample h ,

$$q = c \frac{\Delta p}{h},$$

where the constant c varies with the sand type. Later it was also derived mathematically [31]. The Darcy's law written as a differential equation is

$$\mathbf{q} = -\frac{K_S}{\mu} (\nabla p - \rho \mathbf{g}), \quad (2.11)$$

where K is the permeability, μ the viscosity of the fluid, p is the pressure, ρ the fluid density and \mathbf{g} the gravitation vector.

The permeability K_S in Darcy's law depends on the type of porous media, i.e. the type of rock, or in our case, the kind of concrete. It is a measure on how easily fluids flow through the medium, and is an average property of the medium [9]. For homogeneous and isotropic medium the permeability K_S is a scalar constant [37]. In other cases it will vary throughout the material.

We have two phases, but are just interested in the flow in the water phase. The presence of a gas phase influence the flow of the water phase, and the absolute permeability K_S in eq. (2.11) get multiplied with a relative permeability k . The relative permeability of the water phase depends on the water saturation

$$k = k(\phi_w), \quad (2.12)$$

where as the absolute permeability is a material parameter depending on the medium. We then get the effective permeability for the water phase

$$K = k(\phi_w) K_S, \quad (2.13)$$

which is the reduced permeability due to the presence of a gas phase in addition to the water phase. Darcy's law for the water phase is then

$$\mathbf{q}_w = -\frac{k(\phi_w) K_S}{\mu_w} (\nabla p_w - \rho_w \mathbf{g}). \quad (2.14)$$

Here μ_w denotes the water viscosity, ρ_w the water density and p_w the water pressure. We will assume the model that we only have water flow, and denote in what follows $\mathbf{q} = \mathbf{q}_w$.

When we have the mass conservation equation of water, the flux is given by Darcy's law, that is $\mathbf{v} = \mathbf{q}$. Thus inserting Darcy's law eq. (2.14) into the mass conservation equation (2.10) gives

$$\frac{\partial}{\partial t} (\rho_w \phi \phi_w) - \nabla \cdot \left(\rho_w \frac{k(\phi_w) K_S}{\mu_w} (\nabla p - \rho_w \mathbf{g}) \right) = Q.$$

And further, when we assume the water density ρ_w to be constant, we get

$$\frac{\partial}{\partial t} \phi \phi_w - \nabla \cdot \left(\frac{k(\phi_w) K_S}{\mu_w} (\nabla p - \rho_w \mathbf{g}) \right) = \frac{Q}{\rho_w}. \quad (2.15)$$

2.1.4 Diffusion and transport equations

We will also have mass conservation equations for species in the air and in the water phases in the pores. Letting $u = u(x, t)$ define their concentrations, their mass conservation equations can be given as

$$\frac{\partial u}{\partial t} + \nabla \cdot \mathbf{J} = Q, \quad (2.16)$$

where \mathbf{J} denotes the flux over the boundary of the domain.

A way to picture the flux over the boundary, is if you imagine a window on the boundary where particles pass through. If you can count the number of particles passing through a time interval, then the flux can be defined as the this number of particles divided by the area of the window and the length of the time interval [5]

$$\mathbf{J} = \frac{\text{number of particles passing through window}}{\text{area of window} \times \text{time interval}}.$$

This flow of particles can either be by diffusion or by transport.

Diffusion is the spreading due to molecular movements. The molecules move from areas with high concentration to areas with low concentration by random movements [24]. From experiments the following law is found describing the diffusion

$$\mathbf{J}^{(1)} = -D \nabla u, \quad (2.17)$$

where D is the diffusion coefficient. D is also called the molecular diffusivity [24]. For reactions in solutions, eq. (2.17) is called Fick's first law [5].

For only diffusion and no transport, the conservation equation (2.16) becomes

$$\frac{\partial u}{\partial t} - \nabla \cdot (D \nabla u) = Q. \quad (2.18)$$

When considering concentrations, this equation is called the diffusion equation. The homogeneous version for eq. (2.18), i.e. for $Q = 0$, is called Fick's second law [5].

For a fluid in movement, the particles are transported in this movement. This is given by

$$\mathbf{J}^{(2)} = \mathbf{q}u, \quad (2.19)$$

where \mathbf{q} is the velocity of the fluid which was found from Darcy's law eq. (2.14). Combining diffusion and transport in eq. (2.10), we get the convection-diffusion equation

$$\frac{\partial u}{\partial t} - \nabla \cdot (D \nabla u - \mathbf{q}u) = Q. \quad (2.20)$$

When we consider only transport, we have the transport equation

$$\frac{\partial u}{\partial t} + \nabla \cdot (\mathbf{q}u) = Q. \quad (2.21)$$

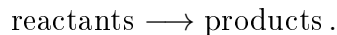
The diffusion equation (2.18) is a second order parabolic partial differential equation, while the transport equation (2.21) is a first order hyperbolic PDE [11]. They have different properties, and also the technique used to solve them differs [16]. Therefore it is important to know if the diffusion or the convection is the dominating process, when we want to solve the convection-diffusion equation (2.20). The strength between the processes is measured by the Péclet number. When convection dominates, we can ignore diffusion, and solve the transport equation (2.21) instead [24]. We will consider examples where the diffusion dominates, thus apply the convection-diffusion equation (2.20) or only the diffusion equation (2.18).

2.2 Chemical reactions

The chemical reactions will provide a sink or a source term, depending on if the species is produced or binded in the reaction. Thus they have to be put into the mass conservation equations in our model. Our reaction involves the reactants CO_2 and $\text{Ca}(\text{OH})_2$, and we get the products CaCO_3 and H_2O .

2.2.1 Reaction rate

A chemical reaction can be written as an equation by



The reaction progress can be followed by either the increase in products, of decrease in reactants [8]. For two reactants, A and B , the reaction rate, which is the rate of the production, is proportional to the concentrations of the to reactants, $[A]$ and $[B]$

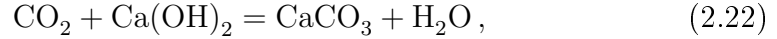
$$\text{rate} = r[A][B],$$

where r is the rate constant. Or the more general version of this rate law is

$$\text{rate} = r[A]^x[B]^y.$$

The parameters r , x and y be found through experiments [8].

Our reaction is the one between carbon dioxide and calcium hydroxide, forming calcium carbonate and water, that is



thus our reactants are CO_2 and Ca(OH)_2 . For concrete carbonation, calcium carbonate is decisive, thus we want to find the rate of the production of CaCO_3

$$\text{rate} = r[\text{CO}_2]^x[\text{Ca(OH)}_2]^y. \quad (2.23)$$

We will let $x = y = 1$.

2.2.2 Dissolution/Precipitation

Precipitation is when a solid forms from a solution [34]. In our case, CaCO_3 is formed in the pore water by concrete carbonation. Thus, first it is fluid, but from the water, it forms into a solid and adds to the solid concrete. This will reduce the porosity of the concrete sample Ω . Precipitation is the opposite of dissolution, when a substance is dissolved into a fluid. Ca(OH)_2 is dissolved into the pore water from the solid concrete.

Papadakis et al [32] include the dissolution. They use results from [40]. For a general definition of dissolution rate, see [15].

Henry's law

Henry's law gives the quantitatively relationship between gas solubility and pressure. It states that "the solubility of a gas in a liquid is proportional to the pressure of the gas over the solution:" [8]

$$c = Hp, \quad (2.24)$$

where c is the molar concentration of the dissolved gas, p is the atmospheric pressure and H is the Henry constant. For more details, see [17, 26].

2.3 The model

The starting point for our numerical study of concrete carbonation, is the article by Radu et al. [39]. Their model is based on the models in Meier et al. [27] and Peter et al. [36], which in turn is based on the model of Papadakis et al. [32]. The models in [27,32,36] all involve mass conservation equations for CO_2 , $\text{Ca}(\text{OH})_2$ and CaCO_3 , as well does the model in [39]. In [27,32,36] they assume that the species only spread because of diffusion, but in [39] they also assume there is water flow transporting the species, in this way, applying the flow equations from reservoir modeling to the concrete carbonation problem. They get a set of coupled equations involving non-linear terms. We will here explain how these equations are derived.

We assume we have a homogeneous porous medium. In our case a volume of reinforced concrete. The initial porosity is then assumed to be constant in the sample. Let A and a denote the concentrations of carbon dioxide as a liquid, $\text{CO}_2(\text{aq})$, and in the air, $\text{CO}_2(\text{g})$, B and b the concentrations of calcium hydroxide in the pore water, $\text{Ca}(\text{OH})_2(\text{aq})$, and in the solid concrete $\text{Ca}(\text{OH})_2(\text{s})$, and C and c denotes the concentrations of $\text{CaCO}_3(\text{aq})$ and $\text{CaCO}_3(\text{s})$ of calcium carbonate. The concentrations are given as number of moles per unit volume. They are measured in mol/L, then called the molar concentration, or more correctly in mol/dm³, e.g. called the amount-of-substance concentration [7].

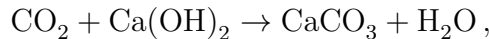
In Radu et al. [39] they define the reaction rate as

$$\gamma = r\phi\phi_w AB, \quad (2.25)$$

letting $x = y = 1$, where A and B are the molar concentrations of CO_2 and $\text{Ca}(\text{OH})_2$ respectively. r is the reaction constant for concrete carbonation, see section 2.2.1. This reaction rate accounted for the influence of the humidity by the water saturation ϕ_w and the geometry of the concrete by the porosity ϕ . Here r is a constant which may have a big value. In their article, Radu et al., further gives the production rates by the reaction as

$$\gamma_i = \sigma_i m_i \gamma, \quad (2.26)$$

for the species $i \in \{A, B, C\}$. For the species i , σ_i is the stoichiometric coefficient of the reaction, balancing the equation of the reaction [5], and m_i is the molecular weight. For our concrete carbonation reaction



we have one carbon C and one calcium Ca atom on each side, four oxygen atoms O and two hydrogen atoms H on each side, thus we don't have to add any coefficients to the chemicals to make the reaction add up, thus for this reaction the stoichiometric coefficients $\sigma_i = 1$ for $i = A, B, C$.

2.3.1 The water flux equations

We will first describe the two first equations involving the water flux \mathbf{q} . These equations are taken from reservoir modeling, see e.g. [9, 37], and come from conservation of water and Darcy's law, eq. (2.11). For the water phase the conservation law is [37]

$$\nabla \cdot (\rho_w \mathbf{q}) + \frac{\partial \rho_w \phi \phi_w}{\partial t} = Q, \quad (2.27)$$

where ρ_w is the water density, \mathbf{q} is the water flux, ϕ the porosity and ϕ_w the water saturation given by eq. (2.3). For constant density ρ_w , eq. (2.27) becomes

$$\rho_w \nabla \cdot \mathbf{q} + \rho_w \frac{\partial \phi \phi_w}{\partial t} = Q,$$

or

$$(\phi \phi_w)_t + \nabla \cdot \mathbf{q} = \frac{Q}{\rho_w}.$$

There is produced water in the reaction of concrete carbonation, thus here Q is a source term given by the reaction rate γ , eq. (2.25). This gives us

$$(\phi \phi_w)_t + \nabla \cdot \mathbf{q} = \frac{\phi \phi_w}{\rho_w} r_{AB}. \quad (2.28)$$

The water flux \mathbf{q} is given by Darcy's law for the water phase [37]

$$\mathbf{q} = \frac{-K_S k(\phi_w)}{\mu_w} (\nabla p_w - \rho_w \mathbf{g}),$$

while we have here

$$\mathbf{q} = -K_S \phi k(\phi_w) \nabla (p + z). \quad (2.29)$$

The differences between these two equations are that the porosity ϕ is added, and the viscosity is not. z covers the gravitation-term, $\nabla z = -\mathbf{g}$. In Radu et al. [39], they assume the air pressure is constant, and $p = -p_c$ the capillary pressure. They also assume the following relation, that the relative k is also a function of the porosity ϕ , and that $k(\phi, \phi_w) = \phi k(\phi_w)$. Viscosity of water is around 1 mPa · s when the water temperature is 20°C. It measures the resistance of water to flow [34]. It has been disregarded here.

When we insert eq. (2.29) into eq. (2.28), we get the pressure equation

$$(\phi \phi_w)_t - \nabla \cdot (K_S \phi k(\phi_w) \nabla (p + z)) = \frac{\phi \phi_w}{\rho_w} r_{AB}, \quad (2.30)$$

where the water saturation is assumed to be a function of the pressure, $\phi_w = \phi_w(p)$. Because water density is the only density we will consider in what follows, we let will denote $\rho = \rho_w$, omitting the index.

2.3.2 The equations of the chemical species

Now we look at the mass conservation equations for the chemical species. We assume that there in the water phase, is both diffusion because of the spreading out of the species, and transport because of the water flowing. In the air phase, there is no transport, only diffusion, and in the solid phase, there is neither diffusion nor transport. There is an interaction between the phases, when a species dissolves into the fluid, either from the solid or from the air. Or when a species forms in the water, and then gets attached to the solid. The reaction happens in the water, thus in the water phase, there will be a source or a sink term, depending on if the species is produced or used in the reaction.

The mass conservation equations for the species are all on the form

$$(\phi\phi_w E)_t + \nabla \cdot (-D_E \phi\phi_w \nabla E + \mathbf{q}E) = Q_i + \gamma_i,$$

where E stands for A , B or C . D_E is the diffusion coefficient of the species, Q_i represents the interchange between the phases for the species of consideration, and γ_i its production rate, eq. (2.26).

For CO_2 in the air, a , we have similar the equation

$$(\phi\phi_g a)_t + \nabla \cdot (-D_a \phi\phi_g \nabla a) = Q_a.$$

The change of carbon dioxide in the air inside the concrete, is only due to the transfer of CO_2 between the air and the water phase. The CO_2 in the air is dissolved into the water, and this provides a sink term for a , the CO_2 in the air, and a source term for the CO_2 in the water. This is covered by a term given from the Henry's law, $P(H\phi\phi_w A - \phi\phi_g a)$, see section 2.2.2. This term express the reduction of CO_2 , thus it has a negative sign in front in the equation for A , CO_2 in water, and a positive sign in the equation for a . We then get,

$$(\phi\phi_w A)_t + \nabla \cdot (-D_A \phi\phi_w \nabla A + \mathbf{q}A) = -P(H\phi\phi_w A - \phi\phi_g a) - r\phi\phi_w m_A AB, \quad (2.31)$$

$$(\phi\phi_g a)_t + \nabla \cdot (-D_a \phi\phi_g \nabla a) = P(H\phi\phi_w A - \phi\phi_g a), \quad (2.32)$$

where the production rate of A also is added.

$\text{Ca}(\text{OH})_2$ dissolves from the solid concrete into the pore water, while CaCO_3 precipitates from the water phase to the solid phase. Radu et al. [39] give this dissolution of $\text{Ca}(\text{OH})_2$ by

$$f_{\text{Diss}} = S_{\text{Diss}}(B_{eq} - B), \quad (2.33)$$

and the precipitation of CaCO_3 as

$$f_{\text{Prec}} = S_{\text{Prec}}(C - C_{eq}), \quad (2.34)$$

where S_{Prec} and S_{Diss} are given constants, and B_{eq} and C_{eq} are known equilibrium profiles of the concentrations of $\text{Ca}(\text{OH})_2$ and CaCO_3 [39].

Then we get the mass conservation equations for calcium hydroxide as

$$(\phi\phi_w B)_t + \nabla \cdot (-D_B\phi\phi_w\nabla B + \mathbf{q}B) = f_{\text{Diss}}\phi\phi_w - r\phi\phi_w m_B AB, \quad (2.35)$$

$$(\phi_s b)_t = -f_{\text{Diss}}\phi_s. \quad (2.36)$$

Similar we get for the concentrations of calcium carbonate in the water and in the solid

$$(\phi\phi_w C)_t + \nabla \cdot (-D_C\phi\phi_w\nabla C + \mathbf{q}C) = -f_{\text{Prec}}\phi\phi_w + r\phi\phi_w m_C AB, \quad (2.37)$$

$$(\phi_s c)_t = f_{\text{Prec}}\phi_s. \quad (2.38)$$

2.3.3 The equation for the porosity

In addition to the diffusion and transport equations, we want to add an equation for the porosity $\phi = \phi(x, t)$. We will assume that the porosity changes, and the equation should cover this change. The two actions changing the porosity is the precipitation of CaCO_3 and the dissolution of $\text{Ca}(\text{OH})_2$. When $\text{Ca}(\text{OH})_2$ dissolves into the pore water, the porosity increases, while it decreases when CaCO_3 precipitates from the water and gets solid. Thus the change in the porosity should be proportional to the precipitation and the negative dissolution. The amounts which precipitates and dissolves, depends also on how much water there are in the pores, that is, on the water saturation ϕ_w . We then should have an equation on the following form

$$\phi_t = c\phi(\phi_w f_{\text{Diss}} - \phi_w f_{\text{Prec}}),$$

for a constant c , where f_{Diss} and f_{Prec} are given by eqs. (2.33) and (2.34).

The following equation for the porosity is given in the article of Radu et al. [39]

$$\phi_t = s(\phi - \delta) \frac{1 - \phi}{Z_\phi + (1 - \phi)} (\phi_w f_{\text{Diss}} - \phi_w f_{\text{Prec}}). \quad (2.39)$$

The variable s is a switcher, allowing us to change between variable and constant porosity. If $s = 1$, then the porosity varies with time, but if $s = 0$, we get $\phi = \phi_I$, the initial porosity, and the porosity is constant. δ and Z_ϕ are two positive regularization parameters.

2.3.4 Simplifications

The exchange of CO₂ between the air and the water phase, is fast [36]. A very fast exchange between these phases, corresponds to $P \rightarrow \infty$ and [39]

$$H\phi_w A \approx \phi_g a,$$

This gives then

$$P(H\phi\phi_w A - \phi\phi_g a) \approx 0,$$

and eq. (2.32) becomes

$$(\phi\phi_g a)_t + \nabla \cdot (-D_a \phi\phi_g \nabla a) = 0,$$

and decouples from the rest of the equations. Because of this rapid transfer of CO₂ across the phases, and because CO₂ mainly diffuses through the air, we should use the diffusion coefficient of CO₂ in air in the mass conservation equation for CO₂, letting $D_A = D_a$ in what follows.

We see directly that eqs. (2.36) and (2.38) for b and c respectively, are independent of the other unknowns, and then also decouples from the rest of the system. In addition we disregard the influence of the gravitation in the equation for the flux eq. (2.29). Then, when we do these simplifications, gives us the reduced system

$$(\phi\phi_w)_t + \nabla \cdot \mathbf{q} = \frac{\phi\phi_w}{\rho} rAB, \quad (2.40)$$

$$\mathbf{q} = -K_S \phi k(\phi_w) \nabla p, \quad (2.41)$$

$$(\phi\phi_w A)_t + \nabla \cdot (-D_A \phi\phi_w \nabla A + \mathbf{q}A) = -r\phi\phi_w m_A AB, \quad (2.42)$$

$$(\phi\phi_w B)_t + \nabla \cdot (-D_B \phi\phi_w \nabla B + \mathbf{q}B) = f_{\text{Diss}} \phi\phi_w - r\phi\phi_w m_B AB, \quad (2.43)$$

$$(\phi\phi_w C)_t + \nabla \cdot (-D_C \phi\phi_w \nabla C + \mathbf{q}C) = -f_{\text{Prec}} \phi\phi_w + r\phi\phi_w m_C AB, \quad (2.44)$$

$$\phi_t = s(\phi - \delta) \frac{1 - \phi}{Z_\phi + (1 - \phi)} (\phi_w f_{\text{Diss}} - \phi_w f_{\text{Prec}}). \quad (2.45)$$

Here we have a set of six equations in eight unknowns $A, B, C, p, \mathbf{q}, \phi, \phi_w$ and k . We need constitutive equation/reasons for ϕ_w and k to close the system. In Radu et al [39] they use the van Genuchten-Mualem parametrization to find an expression for the relative permeability k and the water saturation ϕ_w .

In [48] van Genuchten gives the dimensionless water content as

$$\Theta = \left[\frac{1}{1 + (\alpha h_p)^n} \right]^m, \quad (2.46)$$

and the relative permeability as

$$k(\Theta) = \Theta^{1/2} [1 - (1 - \Theta^{1/m})^m]^2, \quad (2.47)$$

for $m = 1 - 1/n$ and $0 < m < 1$. h_p is the pressure head, $h_p = \rho g$ which is a scaled value of the pressure [31]. The parameters α , m and n can be derived from experimental data.

In [39] this becomes

$$\phi_w(p) = \phi_{w,max} (1 + (-\alpha p)^n)^{-m}, \quad (2.48)$$

$$k(\phi_w) = \sqrt{\phi_w} (1 - (1 - \phi_w^{1/m})^m)^2, \quad (2.49)$$

where

$$m = 1 - \frac{1}{n}.$$

2.3.5 Numerical solution approach

We want to solve this system numerically. The model consists of several equations which are coupled, that is each equation contains several of the unknowns from the other equations. We will here give the strategy of how we want to solve the system. Coupled equations can be solved implicitly, that is all equations together at ones, or explicitly, when we first solve for one equations and then for the next. We will us a combination of these two strategies.

Each equation can also be solved implicitly or explicitly. We will in the next chapter go into the details around the numerical modeling of the system. We will here just give an overview of how we want to do it. First, we will solve explicitly the equation

$$\phi_t = s(\phi - \delta) \frac{1 - \phi}{Z_\phi + (1 - \phi)} (\phi_w f_{\text{Diss}} - \phi_w f_{\text{Prec}}),$$

for the porosity ϕ . Then we use the new value of the porosity to find the pressure p implicitly from

$$(\phi\phi_w)_t + \nabla \cdot (-K_S \phi k(\phi_w) \nabla p) = \frac{\phi\phi_w}{\rho} r_{AB}.$$

Further, from the pressure, we find the water flux \mathbf{q} from

$$\mathbf{q} = -K_S \phi k(\phi_w) \nabla p.$$

The concentration of $\text{CO}_2(\text{aq})$ and $\text{Ca}(\text{OH})_2(\text{aq})$, that is A and B , will we find by solving the equations

$$\begin{aligned} (\phi\phi_w A)_t + \nabla \cdot (-D_A \phi\phi_w \nabla A + \mathbf{q}A) &= -r\phi\phi_w m_{AAB}, \\ (\phi\phi_w B)_t + \nabla \cdot (-D_B \phi\phi_w \nabla B + \mathbf{q}B) &= f_{\text{Diss}}\phi\phi_w - r\phi\phi_w m_{BAB}, \end{aligned}$$

coupled for A and B . And in the end we find the concentration of $\text{CaCO}_3(\text{aq})$ (C) from

$$(\phi\phi_w C)_t + \nabla \cdot (-D_C \phi\phi_w \nabla C + \mathbf{q}C) = -f_{\text{Prec}}\phi\phi_w + r\phi\phi_w m_C AB.$$

We will continue like this for every time-step until we reach the final time-step.

Chapter 3

Numerical modeling

We will solve numerically a set a set of coupled partial and ordinary differential equations in one spatial dimension. To solve these, we will use finite difference methods and two-point flux approximation (TPFA) [3]. In this chapter we will give the theoretical background for the discretization, set up the discretization schemes for the equations, and show how we will couple them together.

3.1 Grid

To solve a mathematical problem numerically, we need to discretize the problem. The same accounts for if you want to represent a mathematical function $f(\mathbf{x})$ numerically, you first have to define the points \mathbf{x}_i for where to calculate the function. Defining those points, is to define a grid on the functions domain.

The way we make the grid, can be thought of as dividing the interval into cells with walls separating the cells. In two-dimensions the grid get generated by putting out several points in the domain, and then connect the points by straight lines not intersecting each other. When we look at the

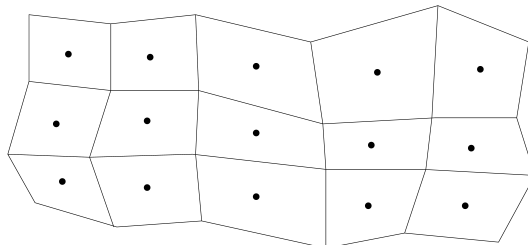


Figure 3.1: An example of a cell-centered grid in 2-d.

grid as containing cells, the lines are the cell walls and the grid points are the corners of the cells. We then can choose the points \mathbf{x}_i to be the same as the grid points, or we can let the points \mathbf{x}_i be the middle points of the cells, giving us a cell-centered grid [2], see fig. 3.1.

For control-volume methods a cell-centered grid is needed, and therefore we choose such a grid. Usually, to define the points \mathbf{x}_i for a cell-centered grid, you have to divide the interval into cells first, then find the middle-point of the cells and let them be the points \mathbf{x}_i [2], but for an equidistant one-dimensional grid, it does not matter if you define the discretization points \mathbf{x}_i or the walls of the cells first.

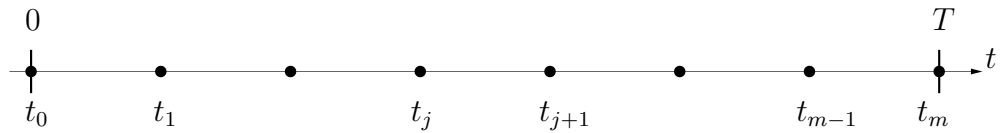


Figure 3.2: Equal distant time discretization

We will have one discretization in time and one in space. Our time interval is $[0, T]$, thus starting time $t_0 = 0$ and T gives the end time $t_m = T$. The size of the time steps are given by $\Delta t_j = t_j - t_{j-1}$. We have equal distance time interval, where time step size is constant $\Delta t_j = \tau$ for $j = 0, \dots, m$. Then τ is found from $\tau = T/m$.

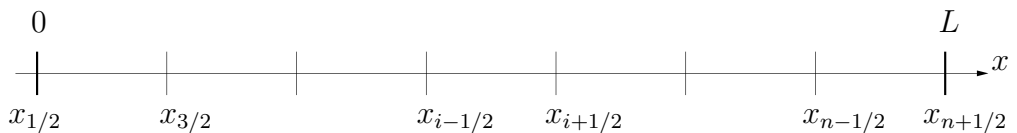


Figure 3.3: Space interval divided into equal sized cells.

We are going to use control-volume method in space, thus we discretization the space interval $[0, L]$ into a cell-centered grid. For the spacing we will just consider equal distance grid. We then start by dividing the interval $[0, L]$ in n equal cells. The walls of the cells are given by $x_{i+1/2} = ih$ for $i = 0, \dots, n$, where $h = x_{i+1/2} - x_{i-1/2} = L/n$. Then $x_{1/2} = 0$ and $x_{n+1/2} = L$ gives the boundaries of the domain, see fig. 3.3.

After dividing the space interval into cells, we take the middle points of the cells to be the grid points x_1, x_2, \dots, x_n , see fig. 3.4. Because we have an

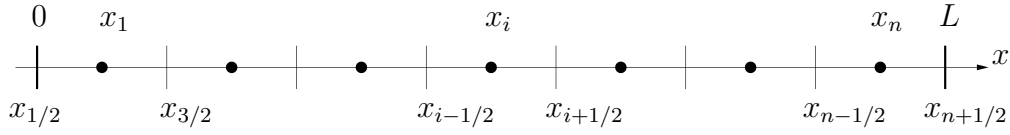


Figure 3.4: Cell-centered space discretization.

equal distant grid, the distance between the neighboring grid points, will be the same as the size of the cells, $\Delta x_i = x_{i+1} - x_i = h$. Then $x_1 = h/2$ and $x_i = ih - h/2$ for $i = 0, \dots, n$. The last grid point is $x_n = nh - h/2 = L - h/2$.

3.2 Spatial discretization

The equations eqs. (2.42) to (2.44) are partial differential equations for x and t , thus we have to discretize them both in space and time. In this section we will look at the space discretization, and boundary conditions. There are several ways to discretize a partial differential equation in space. The method we are going to use, is the two-point flux approximation (TPFA). It is a control volume method. In 1-d it is equivalent to the finite difference method for a cell-centered grid.

3.2.1 Finite difference approximation

The most elementary space discretization method, is the finite difference approximation. It is based on Taylor series taught in elementary calculus courses [4]. The finite difference approximation is described in books on numerical analysis, e.g. [2, 11, 14, 18, 22]. Taylor series and finite difference method is also the basis for the time discretizations eqs. (3.40) and (3.41) in section 3.3.

The finite difference methods are defined from the Taylor series for $u(x+h) = u(x_{i+1})$ and $u(x-h) = u(x_{i-1})$. From the series

$$u(x_{i+1}) = u(x_i) + hu'(x_i) + \frac{h^2}{2}u''(x_i) + \frac{h^3}{3!}u'''(x_i) + \dots, \quad (3.1)$$

we get the forward difference approximation for the first derivative,

$$u'(x_i) = \frac{u(x_{i+1}) - u(x_i)}{h} + O(h). \quad (3.2)$$

The term $O(h)$ gives the order of the method, that is that terms which are truncated from the series, are of order h . Similar we get the backward

difference approximation

$$u'(x_i) = \frac{u(x_i) - u(x_{i-1}))}{h} + O(h), \quad (3.3)$$

from

$$u(x_{i-1}) = u(x_i) - hu'(x_i) + \frac{h^2}{2}u''(x_i) - \frac{h^3}{3!}u'''(x_i) + \dots \quad (3.4)$$

The forward and backward approximations are both of order h , thus they are fairly bad. We get a better approximation by subtracting eq. (3.4) from eq. (3.1). This gives us the central difference approximation

$$u'(x_i) = \frac{u(x_{i+1}) - u(x_{i-1}))}{2h} + O(h^2). \quad (3.5)$$

To get an approximation for the second derivative, we use

$$\frac{u(x_{i+1}) - u(x_i)}{h} = u'(x_i) + \frac{h}{2}u''(x_i) + \frac{h^2}{3!}u'''(x_i) + \frac{h^3}{4!}u^{(4)}(x_i) + \dots, \quad (3.6)$$

$$\frac{u(x_i) - u(x_{i-1}))}{h} = u'(x_i) - \frac{h}{2}u''(x_i) + \frac{h^2}{3!}u'''(x_i) - \frac{h^3}{4!}u^{(4)}(x_i) + \dots \quad (3.7)$$

When we subtract eq. (3.7) from eq. (3.6) we get

$$u''(x_i) = \frac{u(x_{i+1}) - 2u(x_i) + u(x_{i-1}))}{h^2} + O(h^2). \quad (3.8)$$

This is the central difference formula for the second derivative $u''(x_i)$.

3.2.2 Control volume methods

The starting point for the control volume methods, are to lay out a grid on the domain of the differential equation, dividing it into cells like we did in fig. 3.3 for the 1-d case. We call these cells, control volumes, from there the name of the method. The mass conservation principle will then be used in each of these control volumes. This holds when the fluxes on each side of a cell wall are equal [2]. The integral form of the mass conservation equation, eq. (2.9), are then applied to each cell or control volume. The flux is given across the cell walls, averaging the permeability.

Two-point flux approximation

We start with the ordinary differential equation

$$-(Kp_x)_x = Q, \quad (3.9)$$

where $K = K(x)$ can denote the permeability, and Q the source-term. The index denotes the partial derivative with respect to x , $p_x = \partial p / \partial x$. If we let

$$q = -Kp_x \quad (3.10)$$

denote the flux, we get the equation

$$q_x = Q. \quad (3.11)$$

We want to solve this equation for q . We start to discretize by using a

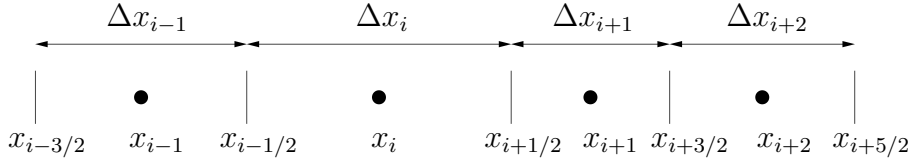


Figure 3.5: Cell-centered grid with grid points x_i and the cell-walls $x_{i+1/2}$.

cell-centered grid in one-dimension, see fig. 3.5. Then the grid points x_i for $i = 0, \dots, n$ are the middle points of the cells. The walls of cell with mid-point x_i are given by $x_{i-1/2}$ and $x_{i+1/2}$. Integrating eq. (3.11) over each cell, we get

$$q_{i+1/2} - q_{i-1/2} = \int_{x_{i-1/2}}^{x_{i+1/2}} Q(x) dx. \quad (3.12)$$

We now want to find an expression for $q_{i+1/2}$ by K and p . To do so we start by rewriting eq. (3.10) as [2]

$$p_x = -\frac{q}{K}. \quad (3.13)$$

Then, when we integrate from middle point x_i to middle point x_{i+1} , we get

$$p_{i+1} - p_i = -q_{i+1/2} \int_{x_i}^{x_{i+1}} \frac{1}{K(x)} dx,$$

and the following expressions of $q_{i+1/2}$ in terms of p_i and p_{i+1} ,

$$q_{i+1/2} = -\frac{p_{i+1} - p_i}{\int_{x_i}^{x_{i+1}} \frac{1}{K(x)} dx}.$$

We now need an approximation of integral

$$\int_{x_i}^{x_{i+1}} \frac{1}{K(x)} dx,$$

from grid point x_i to grid point x_{i+1} . These are the middle points in two neighboring cells, thus we integrate over two cells. We assume that $K(x)$ is constant on each cell, denoted by the values at the grid point, $K_i \approx K(x_i)$. We let Δx_i denote the distance between the walls of the cell, that is $\Delta x_i = x_{i+1/2} - x_{i-1/2}$. We approximate the integral by taking the average over the two cells involving x_i and x_{i+1}

$$\int_{x_i}^{x_{i+1}} \frac{1}{K(x)} dx = \frac{1}{2} \left(\frac{\Delta x_{i+1}}{K_{i+1}} + \frac{\Delta x_i}{K_i} \right).$$

Thus we get the following expression

$$q_{i+1/2} = -\frac{p_{i+1} - p_i}{\frac{1}{2} \left(\frac{\Delta x_{i+1}}{K_{i+1}} + \frac{\Delta x_i}{K_i} \right)}.$$

Which becomes

$$q_{i+1/2} = -a_{i+1}(p_{i+1} - p_i), \quad (3.14)$$

when we let

$$a_i = \frac{1}{\frac{1}{2} \left(\frac{\Delta x_i}{K_i} + \frac{\Delta x_{i-1}}{K_{i-1}} \right)}.$$

This is for a non-equidistant cell-centered grid. For a equidistant cell-centered grid we have $\Delta x_i = h$ for $i = 0, \dots, n$. This gives

$$a_i = \frac{1}{\frac{h}{2} \left(\frac{1}{K_i} + \frac{1}{K_{i-1}} \right)}. \quad (3.15)$$

We will in the rest of the thesis, only consider equidistant, cell-centered grids.

Now, using the expression for q for equidistant, cell-centered grid, eq. (3.12) becomes

$$\frac{p_i - p_{i-1}}{\frac{h}{2} \left(\frac{1}{K_i} + \frac{1}{K_{i-1}} \right)} - \frac{p_{i+1} - p_i}{\frac{h}{2} \left(\frac{1}{K_{i+1}} + \frac{1}{K_i} \right)} = \int_{x_{i-1/2}}^{x_{i+1/2}} Q(x) dx. \quad (3.16)$$

For simplicity, we denote

$$b_i = \int_{x_{i-1/2}}^{x_{i+1/2}} Q(x) dx. \quad (3.17)$$

Then eq. (3.16) can then be written as

$$a_i(p_i - p_{i-1}) - a_{i+1}(p_{i+1} - p_i) = b_i.$$

Rearranging the terms give

$$-a_i p_{i-1} + (a_i + a_{i+1})p_i - a_{i+1}p_{i+1} = b_i. \quad (3.18)$$

for $i = 1, \dots, n$. Thus, we have a system of n equations. The unknowns are $[p_0, p_1, \dots, p_n, p_{n+1}]$. That is, there are $n + 2$ unknowns. To get one unique solution, we need in addition boundary conditions. We will consider Dirichlet and Neumann boundary conditions.

Before we look at how to manage the boundary conditions, we want to compare the discretization scheme we got for using two-point flux approximation eq. (3.18), with the one we get from using finite difference approximation. We let $K_i = K$, a constant for all i , then the finite difference discretization of eq. (3.9) is

$$-K \frac{p_{i+1} - 2p_i + p_{i-1}}{2h} = Q(x_i),$$

from the central difference formula for the second derivative eq. (3.8). This is the same as we get when inserting $a_i = K/h$ into eq. (3.18) and approximating b_i by the midpoint rule, $b_i \approx hQ(x_i)$. We then also know from eq. (3.8) that this is a second order method, that is the error is of $O(h^2)$.

3.2.3 Boundary conditions

For Dirichlet boundary conditions, the value of the function is given at the boundary, while for Neumann boundary conditions, the value of the derivative is given at the boundary. We can also mix Dirichlet and Neumann boundary conditions, by using Dirichlet boundary conditions on one of the boundaries and Neumann on the other boundary.

In the literature, mostly vertex centered grids are considered. For Dirichlet and Neumann boundary conditions on vertex centered grids, see e.g. [11, 18]. Dirichlet and Neumann boundary conditions are in [46] given for cell-centered grids in addition to for vertex centered grids. In [2] they give the scheme of elliptic differential equations are given with homogeneous Dirichlet boundary conditions without getting into details.

Dirichlet boundary conditions

For a differential equation, or a system of differential equations, the Dirichlet boundary conditions are given by the function values of the unknown in the endpoints of the domain. We consider the one-dimensional problem eq. (3.9) on the domain $[0, L]$. This is a stationary equation, that is does not depend

on time. The unknown is the pressure $p = p(x)$. Then the Dirichlet boundary conditions can be given as

$$p(0) = p_O, \quad (3.19)$$

and

$$p(L) = p_L. \quad (3.20)$$

Because we have the cell-centered grid, fig. 3.4, when the problem is discretized,

$$p_{1/2} = p_O,$$

and

$$p_{n+1/2} = p_L.$$

Thus it is not straight forward how to handle Dirichlet boundary conditions for cell-centered grids. For vertex centered grids, the boundary points will coincide with the grids points in the ends. But this is not the case here, and we have to find a way to deal with this problem.

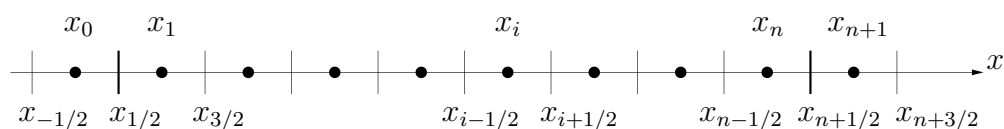


Figure 3.6: Dirichlet boundary conditions for cell-centered grid by adding ghost cells in the ends of the interval.

In [46] they present two ways to handle Dirichlet boundary conditions for cell-centered grids. The first opportunity is to add ghost cells in the ends of the interval as done in fig. 3.6. Then we assume that the Dirichlet boundary conditions are prescribed at the ghost cells and we discretize in the first and the last cell as shown above. We get then the additional grid points x_0 and x_{n+1} , and we assume

$$p_0 = p_O,$$

and

$$p_{n+1} = p_L.$$

They note in [46] that this is a first order approximation which will not be sufficient if the solution depends a lot on the boundary conditions. Another way to do it, is to add half cells at the ends of the interval, see fig. 3.7. We will in what follows use the first approach. We will consider both Dirichlet and Neumann boundary conditions, and when combining them, it seems best to apply ghost cells for the Dirichlet boundary conditions.

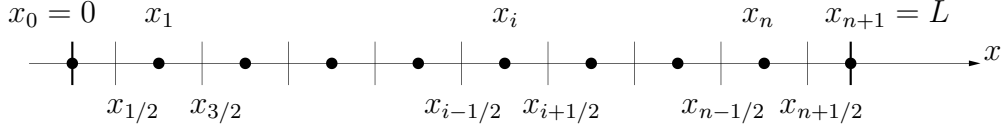


Figure 3.7: Dirichlet boundary conditions for cell-centered grid by adding half cells in the ends of the interval.

When we use the first approach of adding ghost cells, we basically handle the Dirichlet boundary conditions on the same way as we would have done for a vertex centered grid. The difference lays in how we define the grid points x_i and then also in which points we compute the values of p . We show how to manage the boundary conditions for

$$-(Kp_x)_x = Q.$$

where we use the first approach by adding ghost cells in the ends of the interval. We found the discretization in the previous section the discretization of this problem, see eq. (3.18). From this, the system of equations we get looks like

$$\begin{aligned} -a_1p_0 + (a_1 + a_2)p_1 - a_2p_2 &= b_1 \\ -a_2p_1 + (a_2 + a_3)p_2 - a_3p_3 &= b_2 \\ &\vdots \\ -a_{n-1}p_{n-2} + (a_{n-1} + a_n)p_{n-1} - a_np_n &= b_{n-1} \\ -a_np_{n-1} + (a_n + a_{n+1})p_n - a_{n+1}p_{n+1} &= b_n \end{aligned}$$

From the boundary conditions, we have $p_0 = p_O$ and $p_{n+1} = p_L$, thus we can move these terms over to the right hand side of the system. We then get

$$\begin{aligned} (a_1 + a_2)p_1 - a_2p_2 &= b_1 + a_1p_O \\ -a_2p_1 + (a_2 + a_3)p_2 - a_3p_3 &= b_2 \\ &\vdots \\ -a_{n-1}p_{n-2} + (a_{n-1} + a_n)p_{n-1} - a_np_n &= b_{n-1} \\ -a_np_{n-1} + (a_n + a_{n+1})p_n &= b_n + a_{n+1}p_L. \end{aligned}$$

Writing this on matrix-form, we let

$$\mathbf{A} = \begin{bmatrix} a_1 + a_2 & -a_2 & 0 & \cdots & 0 \\ -a_2 & a_2 + a_3 & -a_3 & & \vdots \\ 0 & \ddots & \ddots & \ddots & \vdots \\ \vdots & & -a_{n-1} & a_{n-1} + a_n & -a_n \\ 0 & \cdots & 0 & -a_n & a_n + a_{n+1} \end{bmatrix}$$

and

$$\mathbf{b} = \begin{bmatrix} b_1 + a_1 p_O \\ b_2 \\ \vdots \\ b_{n-1} \\ b_n + a_{n+1} p_L \end{bmatrix}.$$

We want to solve the system

$$\mathbf{A}\mathbf{p} = \mathbf{b},$$

for the $\mathbf{p} = [p_1, p_2, \dots, p_{n-1}, p_n]^T$. This is a linear system which can be solved by use of a numerical linear solver.

Neumann boundary conditions

We will now look at the case where we have Neumann boundary conditions. When we have Neumann boundary conditions, the values of the first derivative of the function are given at the boundaries. That is, the boundary conditions in the 1-dimensional case is given as

$$p_x(0) = p_\alpha, \quad (3.21)$$

and

$$p_x(L) = p_\beta. \quad (3.22)$$

Again $x_{1/2} = 0$ and $x_{n+1/2} = L$, figs. 3.4 and 3.6. And because $q_{i+1/2}$ express the derivative of the pressure p at the cell wall $x_{i+1/2}$, we can write the boundary conditions as

$$q_{1/2} = -\frac{p_\alpha}{\frac{1}{2} \left(\frac{1}{K_0} + \frac{1}{K_1} \right)},$$

and

$$q_{n+1/2} = -\frac{p_\beta}{\frac{1}{2} \left(\frac{1}{K_n} + \frac{1}{K_{n+1}} \right)}.$$

Since we do not know the values of K_0 and K_{n+1} , but we will assume $K_0 = K_1$ and $K_n = K_{n+1}$. We will in what follows only consider homogeneous Neumann conditions, that is $p_\alpha = p_\beta = 0$. This gives us

$$q_{1/2} = 0, \quad (3.23)$$

and

$$q_{n+1/2} = 0, \quad (3.24)$$

and we do not need values for K_0 and K_{n+1} .

We will now again show how to deal with Neumann boundary conditions for the discretization of eq. (3.9)

$$-(Kp_x)_x = Q.$$

We use the previous discretization. From eq. (3.12) and eq. (3.17), we have

$$q_{i+1/2} - q_{i-1/2} = b_i,$$

for $i = 1, \dots, n$. For the first equation, when $i = 1$, we get

$$q_{3/2} - q_{1/2} = b_1.$$

Here, we can insert the boundary condition at $x = 0$ eq. (3.23), which gives

$$q_{3/2} = b_1.$$

Similar, the last equation, for $i = n$ eq. (3.24), becomes

$$-q_{n-1/2} = b_n.$$

When we in addition use the fact that

$$q_{i+1/2} = -a_{i+1}(p_{i+1} - p_i),$$

the first equation and the last equation become

$$\begin{aligned} a_2 p_1 - a_2 p_2 &= b_1, \\ -a_n p_{n-1} + a_n p_n &= b_n. \end{aligned}$$

The other equations are the same as before. We can again write the systems of equations as a matrix equation

$$\mathbf{A}\mathbf{p} = \mathbf{b},$$

where this time

$$\mathbf{A} = \begin{bmatrix} a_2 & -a_2 & 0 & \cdots & 0 \\ -a_2 & a_2 + a_3 & -a_3 & & \vdots \\ 0 & \ddots & \ddots & \ddots & \vdots \\ \vdots & & -a_{n-1} & a_{n-1} + a_n & -a_n \\ 0 & \cdots & 0 & -a_n & a_n \end{bmatrix}$$

and

$$\mathbf{b} = \begin{bmatrix} b_1 \\ b_2 \\ \vdots \\ b_{n-1} \\ b_n \end{bmatrix}.$$

Again we will solve the linear system for $\mathbf{p} = [p_1, p_2, \dots, p_{n-1}, p_n]^T$.

When we have homogeneous Neumann boundary conditions, $p_\alpha = p_\beta = 0$, and \mathbf{b} simplifies to $\mathbf{b} = [b_1, b_2, \dots, b_{n-1}, b_n]^T$.

3.2.4 Diffusion-advection equation

We have only looked at a second order ordinary differential equation in space eq. (3.9), but eqs. (2.40) and (2.42) to (2.44) are second order partial differential equations. Equations (2.42) to (2.44) are all on the following form

$$(Su)_t + (-D_u K u_x + q(x, t)u)_x = Q(x, t), \quad (3.25)$$

where $q(x, t)$ is the flux, $Q(x, t)$ the source or sink term, and $u = u(x, t)$ the concentration of a species A , B or C , standing for $\text{CO}_2(\text{aq})$, $\text{Ca}(\text{OH})_2(\text{aq})$ and $\text{CaCO}_3(\text{aq})$, see section 2.3. D_u is a constant depending on the species u , and S and K are some functions

$$S = S(x, t, p(x, t)) \quad (3.26)$$

and

$$K = K(x, t, p(x, t)). \quad (3.27)$$

We start by denoting a variable D as

$$D(x, t) = D_u K(x, t, p(x, t)), \quad (3.28)$$

and by letting

$$d = -D u_x. \quad (3.29)$$

Then eq. (3.25) becomes

$$(Su)_t + d_x + (qu)_x = Q, \quad (3.30)$$

from the linearity of the derivative.

We apply again a cell-centered grid with grid points x_i for $i = 1, \dots, n$, see fig. 3.4. We integrate over each cell $[x_{i-1/2}, x_{i+1/2}]$ in the cell-centered grid, and get

$$\int_{x_{i-1/2}}^{x_{i+1/2}} (Su)_t dx + d_{i+1/2} - d_{i-1/2} + q_{i+1/2}u_{i+1/2} - q_{i-1/2}u_{i-1/2} = \int_{x_{i-1/2}}^{x_{i+1/2}} Q dx, \quad (3.31)$$

where e.g. $d_{i+1/2} = d(x_{i+1/2}, t, p(x_{i+1/2}, t))$ and $u_{i+1/2} = u(x_{i+1/2}, t)$.

The integral on the right hand side of eq. (3.31) need to be found or approximated. We are going to use the midpoint rule or formula [38]. Because x_i is the midpoint in the interval $[x_{i-1/2}, x_{i+1/2}]$ and the length of the interval is h , the rule give

$$\int_{x_{i-1/2}}^{x_{i+1/2}} Q(x, t) dx \approx hQ(x_i, t). \quad (3.32)$$

Similar we get the approximation

$$\int_{x_{i-1/2}}^{x_{i+1/2}} (S(x, t, p)u(x, t))_t dx \approx h(S(x_i, t, p_i)u_i)_t, \quad (3.33)$$

where $u_i = u(x_i, t)$ and $p_i = p(x_i, t)$. Inserting this into eq. (3.31), gives

$$h(S(x_i, t, p_i)u_i)_t + d_{i+1/2} - d_{i-1/2} + q_{i+1/2}u_{i+1/2} - q_{i-1/2}u_{i-1/2} = hQ(x_i, t). \quad (3.34)$$

We do not know the values at the walls of the cells. To find them we use the average of the values in the center of the two neighboring cells. From eq. (3.14) we have

$$q_{i+1/2} = -a_{i+1}(p_{i+1} - p_i) \quad i = 0, \dots, n,$$

where a_i is given from eq. (3.15) for $i = 0, \dots, n + 1$. We approximate $u_{i+1/2}$ by the average

$$u_{i+1/2} \approx \frac{u_i + u_{i+1}}{2}, \quad (3.35)$$

for $i = 0, \dots, n$. This gives

$$q_{i+1/2} u_{i+1/2} - q_{i-1/2} u_{i-1/2} \approx q_{i+1/2} \frac{u_i + u_{i+1}}{2} - q_{i-1/2} \frac{u_{i-1} + u_i}{2},$$

for $i = 1, \dots, n$. Further after multiplying the fractions and do the subtraction, we get

$$q_{i+1/2}u_{i+1/2} - q_{i-1/2}u_{i-1/2} \approx \frac{1}{2} (q_{i+1/2}u_{i+1} + (q_{i+1/2} - q_{i-1/2})u_i - q_{i-1/2}u_{i-1}).$$

Integrating $u_x = -d/D$ we get when the length of each cell is h ,

$$u_{i+1} - u_i = -d_{i+1/2} \frac{h}{2} \left(\frac{1}{D_i} + \frac{1}{D_{i+1}} \right), \quad (3.36)$$

which gives

$$d_{i+1/2} = -\frac{u_{i+1} - u_i}{\frac{h}{2} \left(\frac{1}{D_i} + \frac{1}{D_{i+1}} \right)}. \quad (3.37)$$

This means that

$$d_{i+1/2} - d_{i-1/2} = -\frac{u_{i+1} - u_i}{\frac{h}{2} \left(\frac{1}{D_i} + \frac{1}{D_{i+1}} \right)} + \frac{u_i - u_{i-1}}{\frac{h}{2} \left(\frac{1}{D_i} + \frac{1}{D_{i-1}} \right)},$$

and further by letting

$$c_i = \frac{1}{\frac{h}{2} \left(\frac{1}{D_{i-1}} + \frac{1}{D_i} \right)}, \quad (3.38)$$

we can write it simply as

$$d_{i+1/2} - d_{i-1/2} = -c_{i+1} (u_{i+1} - u_i) + c_i (u_i - u_{i-1}).$$

We get the following scheme

$$\begin{aligned} & h(S(x_i, p)u_i)_t + c_i (u_i - u_{i-1}) - c_{i+1} (u_{i+1} - u_i) \\ & + \frac{1}{2} (q_{i+1/2}u_{i+1} + (q_{i+1/2} - q_{i-1/2})u_i - q_{i-1/2}u_{i-1}) = hQ(x_i, t). \end{aligned}$$

This can be written as

$$\begin{aligned} & h(S(x_i, t, p_i)u_i)_t + \left(-c_{i+1} + \frac{q_{i+1/2}}{2} \right) u_{i+1} \\ & + \left(c_i + c_{i+1} + \frac{q_{i+1/2} - q_{i-1/2}}{2} \right) u_i - \left(c_i + \frac{q_{i-1/2}}{2} \right) u_{i-1} = hQ(x_i, t). \end{aligned}$$

Further, dividing the equation by h , gives

$$\begin{aligned} & (S(x_i, t, p_i)u_i)_t + \frac{1}{h} \left(-c_{i+1} + \frac{q_{i+1/2}}{2} \right) u_{i+1} \\ & + \frac{1}{h} \left(c_i + c_{i+1} + \frac{q_{i+1/2} - q_{i-1/2}}{2} \right) u_i - \frac{1}{h} \left(c_i + \frac{q_{i-1/2}}{2} \right) u_{i-1} = Q(x_i, t). \end{aligned} \quad (3.39)$$

This now a first order ordinary differential equation in time, and we need to discretize the equation in time before we got a system of equations we can solve for u_i , $i = 1, \dots, n$.

3.3 Temporal discretization

We consider now first the ordinary differential equation

$$u'(t) = f(t, u(t)).$$

When we set up the numerical scheme for this equation from the forward difference approach eq. (3.2), we get the forward Euler scheme, called Euler's method [22]

$$u^j = u^{j-1} + \tau f(t_{j-1}, u^{j-1}). \quad (3.40)$$

If we instead use the backwards difference approximation eq. (3.3), we get the backward Euler scheme, or the implicit Euler's method [22],

$$u^j = u^{j-1} + \tau f(t_j, u^j). \quad (3.41)$$

We have here let u^j denote the approximated value of the exact solution u at the time t_j . The index j denotes the time steps, $j = 1, \dots$. τ is the uniform size of the time steps.

We see that the only difference between these two methods, is the input of the function f , and this gives what kind of method it is, if it is an explicit or implicit method. The forward Euler method is an explicit method because when we evaluate the value of the function f in this method, we use the values of the previous step, which are known. On the contrary the backward Euler scheme is an implicit scheme, using the new value u^{j+1} to find the value of the right hand side f .

Both the explicit and implicit Euler methods eqs. (3.40) and (3.41) are first order methods [14]. This is shown from the fact that they are Taylor methods of order 1 [22]. On the other hand, their stability conditions differ [22,38]. The forward Euler scheme is only stable for some values of τ , while the backward Euler scheme is stable for all τ . We will therefore use backward Euler in our simulations. This method is some what more difficult than using the explicit method, forward Euler. If f is not a linear function in u , we need to use a linearization technique, e.g. Newton method, when solving eq. (3.41). Otherwise, if f is a linear function of u , do we have to rearrange the equation on the usual manner to have u^{j+1} alone on one side of the equation.

We now want to use the implicit Euler's method eq. (3.41) to set up the numerical scheme for the diffusion-advection equation eq. (3.25). We have already discretized in space, and got eq. (3.39)

$$\begin{aligned} (S(x_i, t, p_i)u_i)_t + \frac{1}{h} \left(-c_{i+1} + \frac{q_{i+1/2}}{2} \right) u_{i+1} \\ + \frac{1}{h} \left(c_i + c_{i+1} + \frac{q_{i+1/2} - q_{i-1/2}}{2} \right) u_i - \frac{1}{h} \left(c_i + \frac{q_{i-1/2}}{2} \right) u_{i-1} = Q(x_i, t). \end{aligned}$$

In this case

$$f_i(t, u(t)) = Q(x_i, t) - \frac{1}{h} \left(-c_{i+1} + \frac{q_{i+1/2}}{2} \right) u_{i+1} \\ - \frac{1}{h} \left(c_i + c_{i+1} + \frac{q_{i+1/2} - q_{i-1/2}}{2} \right) u_i + \frac{1}{h} \left(c_i + \frac{q_{i-1/2}}{2} \right) u_{i-1},$$

and the approximation of the time derivative is

$$(S(x_i, t, p_i)u_i)_t \approx \frac{S_i^j u_i^j - S_i^{j-1} u_i^{j-1}}{\tau}, \quad (3.42)$$

where $S_i^j = S(x_i, t^j, p(x_i, t^j))$. This gives use the implicit scheme for time step j as

$$s \left(-c_{i+1}^j + \frac{q_{i+1/2}^j}{2} \right) u_{i+1}^j + s \left(c_i^j + c_{i+1}^j + \frac{q_{i+1/2}^j - q_{i-1/2}^j}{2} + S_i^j \right) u_i^j \\ - s \left(c_i^j + \frac{q_{i-1/2}^j}{2} \right) u_{i-1}^j = \tau Q(x_i, t^j) + S_i^{j-1} u_i^{j-1}, \quad (3.43)$$

for $i = 1, \dots, n$. Here we let $s = \tau/h$.

We could have written this more generally, and give a function

$$G = G(x, t, p(x, t), u(x, t))$$

which is a function of u . Then backward Euler gives

$$G_t \approx \frac{G_i^j - G_i^{j-1}}{\tau}. \quad (3.44)$$

In the case we have looked at in this section,

$$G = S(x, t, p(x, t))u(x, t).$$

Thus G is here a linear function of u , and we can discretize as shown above. But if G is nonlinear in u , we need to linearize with the use of e.g. Newton method. We are going to look at this case in the next section.

3.4 Nonlinear equations

Nonlinear equations or systems of nonlinear equations, can not be solved directly by linear methods, and need to be linearized. Common methods are

the fix point method and Newton method. We tried first with the fix point method, but found that the Newton method worked better in our case.

When we assume the water saturation ϕ_w or/and k are nonlinear functions of the pressure p , eq. (2.30) becomes a nonlinear equation for p . We want to solve it implicit in time, and will use the Newton method to linearize the equation.

We will here show the method for the more general equation

$$S(p)_t - K(x, t)p_{xx} = Q(x, t) \quad (t \geq 0, \quad 0 \leq x \leq L), \quad (3.45)$$

which is an extension of eq. (3.9). The inhomogeneous initial condition is

$$p(x, 0) = p_I(x) \quad (0 \leq x \leq L), \quad (3.46)$$

and the inhomogeneous Dirichlet boundary conditions are

$$\begin{aligned} p(0, t) &= p_O \quad (t \geq 0) \\ p(1, t) &= p_L \quad (t \geq 0) \end{aligned} \quad (3.47)$$

where p_O and p_L are scalars. Further do we let S be a nonlinear function of p . From eqs. (3.18) and (3.44) the discretization of eq. (3.45) is

$$S(p_i^j) - sa_i^j p_{i-1}^j + s(a_i^j + a_{i+1}^j)p_i^j - sa_{i+1}^j p_{i+1}^j = \tau Q_i^j + S(p_i^{j-1}),$$

for $i = 1, \dots, n$, where again $s = \tau/h$ and from eq. (3.15)

$$a_i^j = \frac{1}{\frac{h}{2} \left(\frac{1}{K_i^j} + \frac{1}{K_{i-1}^j} \right)}.$$

We treat the Dirichlet boundary, eq. (3.47), same way as we did in section 3.2.3, that is we add them on the right hand of the first and last equation. We then get the following system of equations,

$$\begin{aligned} S_1^j + s(a_1^j + a_2^j)p_1^j - sa_2^j p_2^j &= \tau Q_1^j + S_1^{j-1} + sa_1^j p_O^j \\ S_2^j - sa_2^j p_1^j + s(a_2^j + a_3^j)p_2^j - sa_3^j p_3^j &= \tau Q_2^j + S_2^{j-1} \\ &\vdots \\ S_{n-1}^j - sa_{n-1}^j p_{n-2}^j + s(a_{n-1}^j + a_n^j)p_{n-1}^j - sa_n^j p_n^j &= \tau Q_{n-1}^j + S_{n-1}^{j-1} \\ S_n^j - sa_n^j p_{n-1}^j + s(a_n^j + a_{n+1}^j)p_n^j &= \tau Q_n^j + S_n^{j-1} + sa_{n+1}^j p_L. \end{aligned}$$

Using the Newton method we want to find a solution

$$\mathbf{p}^j = [p_1^j, p_2^j, \dots, p_n^j]^T,$$

for every time step j , such that $\mathbf{F}(\mathbf{p}^j) = 0$. We let $\mathbf{F}(\mathbf{p}^j) = \mathbf{F}^j$, where

$$\mathbf{F}^j = [F_1^j, F_2^j, \dots, F_n^j]^T.$$

The equations are given from eq. (3.45) when $S_i^j = S(p_i^j)$, as

$$\begin{aligned} F_1^j &= S_1^j + s(a_1^j + a_2^j)p_1^j - sa_2^j p_2^j - \tau Q_1^j - S_1^{j-1} - sa_1^j p_O, \\ F_2^j &= S_2^j - sa_2^j p_1^j + s(a_2^j + a_3^j)p_2^j - sa_3^j p_3^j - \tau Q_2^j - S_2^{j-1}, \\ &\vdots \\ F_{n-1}^j &= S_{n-1}^j - sa_{n-1}^j p_{n-2}^j + s(a_{n-1}^j + a_n^j)p_{n-1}^j - sa_n^j p_n^j - \tau Q_{n-1}^j - S_{n-1}^{j-1}, \\ F_n^j &= S_n^j - sa_n^j p_{n-1}^j + s(a_n^j + a_{n+1}^j)p_n^j - \tau Q_n^j - S_n^{j-1} - sa_{n+1}^j p_L^j. \end{aligned}$$

The Newton method is an iterative method. We will iterate for the iteration steps k for $k \geq 1$ until the error is small enough, or until we reach maximum iterations steps. The last is when the method does not converge.

We need the Jacobian matrix at each time step. We let $J_{\mathbf{F}}^j$ denote the Jacobian matrix at time step j ,

$$J_{\mathbf{F}}^j = \begin{bmatrix} \frac{\partial F_1^j}{\partial p_1^j} & \frac{\partial F_1^j}{\partial p_2^j} & \dots & \frac{\partial F_1^j}{\partial p_n^j} \\ \frac{\partial F_2^j}{\partial p_1^j} & \frac{\partial F_2^j}{\partial p_2^j} & & \vdots \\ \vdots & & \ddots & \\ \frac{\partial F_n^j}{\partial p_1^j} & \dots & & \frac{\partial F_n^j}{\partial p_n^j} \end{bmatrix}.$$

From the expressions of F_i^j for $i = 1, \dots, n$, we see that the only nonzero partial derivatives are

$$\begin{aligned} (J_{\mathbf{F}}^j)_{i,i-1} &= \left(\frac{\partial F_i^j}{\partial p_{i-1}^j} \right) = -sa_i^j, \\ (J_{\mathbf{F}}^j)_{i,i+1} &= \left(\frac{\partial F_i^j}{\partial p_{i+1}^j} \right) = -sa_{i+1}^j, \\ (J_{\mathbf{F}}^j)_{i,i} &= \left(\frac{\partial F_i^j}{\partial p_i^j} \right) = S'(p_i^j) + s(a_i^j + a_{i+1}^j). \end{aligned}$$

The expression for $(J_{\mathbf{F}}^j)_{i,i-1}$ holds for $i = 2, \dots, n$, $(J_{\mathbf{F}}^j)_{i,i+1}$ for $i = 1, \dots, n-1$ and $(J_{\mathbf{F}}^j)_{i,i}$ holds for $i = 1, \dots, n$.

The method works for each time step as following: We start with an initial guess

$$\mathbf{p}^j = \mathbf{p}^{j,0}.$$

For the first time step, $j = 1$, we choose the initial condition p_I to be the initial guess for the Newton method. And for the other time steps, we let the initial guesses be the solutions of the previous time steps. If we denote \mathbf{p}_I denote the initial values at each discretizing points, that is $\mathbf{p}_I = [p_I(x_1), p_I(x_2), \dots, p_I(x_n)]^T$, then

$$\mathbf{p}^{1,0} = \mathbf{p}_I.$$

Further, for $j > 2$,

$$\mathbf{p}^{j,0} = \mathbf{p}^{j-1},$$

where \mathbf{p}^{j-1} is the solution found at the previous time step.

For each $k \geq 0$, we start by solving the linear system

$$J_{\mathbf{F}}^j(\mathbf{p}^{j,k})\delta^{j,k} = -\mathbf{F}(\mathbf{p}^{j,k}),$$

for $\delta^{j,k}$. Then, when we have found $\delta^{j,k}$, we let a new approximated value of \mathbf{p}^j be

$$\mathbf{p}^{j,k+1} = \mathbf{p}^{j,k} + \delta^{j,k}.$$

We continue doing this, until either the stopping criteria or maximum iteration steps are reached.

There are two kinds of stopping criteria [38]. One by checking the residual and the other by checking the increment. In both cases, we choose a fixed tolerance ε of the approximated solution. When we use the residual as stopping criteria, we end the iterations at time step j , when $\|\mathbf{F}(\mathbf{p}^{j,k})\| < \varepsilon$. While when we control the increment, we end the Newton iteration when $\|\mathbf{p}^{j,k} - \mathbf{p}^{j,k-1}\| < \varepsilon$, that is, checking if the too last approximations are as close as we want them to be.

We noted that the Newton iterations also can be stopped when it reaches a set maximal number of iteration steps. This is to prevent the method to continue forever if it does not converge. What is important, is to choose the maximal number of steps big enough to be sure to get as good approximation as you want, before you reach maximal iteration steps and the method terminates.

3.5 Coupling the equations

Each of the differential equations we consider, give rise to a set of algebraic equations as seen previous in this chapter. The linear ones will be solved by solving matrix equations similar to those in section.... Assume we have N

such sets of equations, solving for $u_i = [u_{i,1}, u_{i,2}, \dots, u_{i,n}]^T$. If we want to solve all of these systems by one linear system

$$\mathbf{A}u = \mathbf{b},$$

where \mathbf{A} denotes the matrix holding values of the matrices for the separate linear systems. If we have N systems, which solutions are given by

$$\begin{aligned} \mathbf{A}^1 u^1 &= \mathbf{b}^1, \\ \mathbf{A}^2 u^2 &= \mathbf{b}^2, \\ &\vdots \\ \mathbf{A}^N u^N &= \mathbf{b}^N. \end{aligned}$$

Then

$$\mathbf{A} = \begin{bmatrix} \mathbf{A}_{1,1} & \mathbf{A}_{1,2} & \mathbf{0} & \cdots & & \mathbf{0} \\ \mathbf{A}_{2,1} & \mathbf{A}_{2,2} & \mathbf{A}_{2,3} & & & \vdots \\ \mathbf{0} & \mathbf{A}_{3,2} & \mathbf{A}_{3,3} & \mathbf{A}_{3,4} & & \vdots \\ \vdots & & \ddots & \ddots & \ddots & \\ \vdots & & & \mathbf{A}_{n-2,n-2} & \mathbf{A}_{n-1,n-1} & \mathbf{A}_{n-1,n} \\ \mathbf{0} & \cdots & & \mathbf{0} & \mathbf{A}_{n,n-1} & \mathbf{A}_{n,n} \end{bmatrix}$$

where the block-matrices $\mathbf{A}_{i,j}$ are given by

$$\mathbf{A}_{i,j} = \begin{bmatrix} A_{i,j}^1 & 0 & \cdots & 0 \\ 0 & A_{i,j}^2 & 0 & \vdots \\ \vdots & & \ddots & 0 \\ 0 & \cdots & 0 & A_{i,j}^N \end{bmatrix}$$

and $\mathbf{0}$ is the zero matrix in $\mathbb{R}^{N,N}$. When the matrices \mathbf{A}^k , $k = 1, \dots, N$, are in $\mathbb{R}^{n,n}$, then $\mathbf{A} \in \mathbb{R}^{Nn,Nn}$. Further

$$\mathbf{b} = \begin{bmatrix} \mathbf{b}_1 \\ \mathbf{b}_2 \\ \vdots \\ \mathbf{b}_n \end{bmatrix}$$

where

$$\mathbf{b}_k = \begin{bmatrix} b_k^1 \\ b_k^2 \\ \vdots \\ b_k^N \end{bmatrix},$$

holding the element number k in the vectors $\mathbf{b}^1, \mathbf{b}^2, \dots, \mathbf{b}^N$. The solutions are then given in the vector

$$u = [u_1^1, u_1^2, \dots, u_1^N, u_2^1, u_2^2, \dots, u_2^N, \dots, u_n^1, u_n^2, \dots, u_n^N]^T .$$

That is, instead of solving each linear system separately, we solve them all together simultaneously. When the N systems are independent of each other, these two ways of solving them, such give exactly the same solution.

When the systems of equations depend on each other, this has to be taken into account. Equations or systems dependent of each other, can either be solved sequentially or simultaneously. When we solve them sequentially, we solve first one equation or system its unknown using the old values of the other unknowns. When time is involved, we solve the equations like this for every time step, using the values from the previous time step for the unknowns we have not solved for yet at that time step. When we solve them simultaneously, we want to solve them together analogously to what can be done for the independent systems of equations. We can do this with the use of Newton method, which anyway should be used if they are nonlinear, or we can just iterate for every time step, solving first one of the unknowns than the other(s) until the solutions are good “enough”.

3.6 Discretization of the set of equations

The set of equations we are going to solve numerically, is given in the previous chapter by eqs. (2.40) to (2.45). This is a coupled set of equations. We discretize it in time t , and one space dimension x . This give us two dimensions, time and space. In this case, we write the equations in the following way

$$(\phi\phi_w)_t + q_x = \frac{\phi\phi_w}{\rho} rAB, \quad (3.48)$$

$$q = -K_S\phi k(\phi_w)p_x, \quad (3.49)$$

$$(\phi\phi_w A)_t + (-D_A\phi\phi_w A_x + qA)_x = -r\phi\phi_w m_A AB, \quad (3.50)$$

$$(\phi\phi_w B)_t + (-D_B\phi\phi_w B_x + qB)_x = f_{\text{Diss}}\phi\phi_w - r\phi\phi_w m_B AB, \quad (3.51)$$

$$(\phi\phi_w C)_t + (-D_C\phi\phi_w C_x + qC)_x = -f_{\text{Prec}}\phi\phi_w + r\phi\phi_w m_C AB, \quad (3.52)$$

$$\phi_t = s(\phi - \delta) \frac{1 - \phi}{Z_\phi + (1 - \phi)} (\phi_w f_{\text{Diss}} - \phi_w f_{\text{Prec}}) . \quad (3.53)$$

Recall, A , B and C denotes the concentrations of carbon dioxide, calcium hydroxide and calcium carbonate in the water phase. p denotes the pressure,

and q the water flux. For an explanation of the rest of the variables, see section 2.3.

Next to these equations, the water saturation ϕ_w is given as a nonlinear a nonlinear function in p ,

$$\phi_w = \phi_w(p), \quad (3.54)$$

and the relative permeability k is a function of the water saturation,

$$k = k(\phi_w). \quad (3.55)$$

Note that because the water saturation is a function of p , the relative permeability can also be expressed as a function of the pressure p , that is $k = k(p)$. Then, when the equation for the water flux, eq. (3.49), is inserted into the mass conservation equation 3.48, eq. (3.48) becomes an equation which can be solved of p ,

$$(\phi\phi_w(p))_t + (-K_S\phi k(p)p_x)_x = \frac{\phi\phi_w(p)}{\rho}rAB. \quad (3.56)$$

Equations (3.50) to (3.53) and (3.56) form a coupled set of equations. We could have solved them all together at once in one system, as discussed in section 3.5, but we will solve them in separate systems. They will all be discretized in space using the cell-centered grid described in section 3.1, for $x \in [0, 1]$ and the grid points x_1, x_2, \dots, x_n . This grid is shown again here in fig. 3.8.

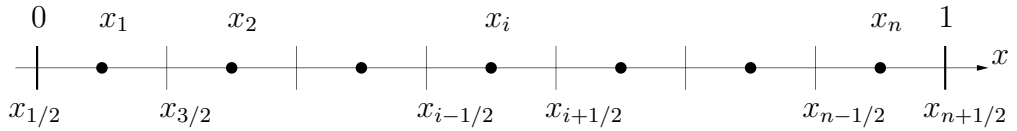


Figure 3.8: Cell-centered space discretization for $x \in [0, 1]$ and the grid points x_1, x_2, \dots, x_n .

Starting with the initial values, ϕ_I, p_I, A_I, B_I and C_I , we will find the solutions of ϕ, p, A, B and C at every time-step for $t = t_1, t_2, \dots, T, t_{j+1} - t_j = \tau$. For every time-step $j > 0$, we will first find the porosity ϕ^j . The porosity is found from eq. (3.53) which is solved implicitly by use of the backward Euler scheme eq. (3.41) given in section 3.3. Thus when we assume variable porosity, $s = 1$, ϕ_i^j is found from

$$\phi_i^j = \phi_i^{j-1} + \tau(\phi_i^{j-1} - \delta) \frac{1 - \phi_i^{j-1}}{Z_\phi + (1 - \phi_i^{j-1})} \phi_{w,i}^{j-1} (f_{\text{Diss},i}^{j-1} - f_{\text{Prec},i}^{j-1}), \quad (3.57)$$

for $i = 1, \dots, n$. Where we use the values of B and C at the previous time-step, $j - 1$, to find f_{Diss}^{j-1} and f_{Prec}^{j-1} . Similarly, ϕ_w^{j-1} is found using p^{j-1} . For constant porosity, $\phi^j = \phi_I$ for all j .

Next, we will find the pressure p^j from eq. (3.56). Because ϕ_w is assumed to be a nonlinear function of p , the pressure equation is here a nonlinear equation, which gives us a nonlinear system of equations when discretized in space. It will be solved semi-implicitly using the following scheme

$$\frac{\phi^j \phi_w^j - \phi^{j-1} \phi_w^{j-1}}{\tau} - (K_S \phi^j k(\phi_w^{j-1}) p_x^j)_x = \frac{\phi^j \phi_w^{j-1}}{\rho} r A^{j-1} B^{j-1},$$

where we use the value of p at the previous time-step to find the permeability and for the water flux in the source term on the right hand side. Then the only nonlinear term we have to consider for p^j , is $\phi^j \phi_w^j$. We will solve this system using Newton method as shown in section 3.4. In this case of the functions S , K and Q in eq. (3.45), we have $S = \phi \phi_w(p)$, $K = K_S \phi k$ and $Q = \frac{\phi \phi_w}{\rho} r AB$. As we did in section 3.4, we assume constant Dirichlet boundary conditions $p(0, t) = p_O$ and $p(1, t) = p_L$. The stopping criteria we use for Newton method, is $\|\mathbf{p}^{j,k} - \mathbf{p}^{j,k-1}\| < 10^{-6}$, and we do max 2000 iteration steps.

When we have found p^j , we proceed by finding A^j and B^j . The equations for A and B , eqs. (3.50) and (3.51), are coupled through the reaction rate $\gamma = r \phi \phi_w AB$. We will solve these two equations together, and use Newton method to do so. Given the discretization of the diffusion-advection equation as described in sections 3.2.4 and 3.3, the entries in the Jacobian matrix for the equations of A , is given as

$$\begin{aligned} \left(\frac{\partial F_{A,i}^j}{\partial A_{i-1}^j} \right) &= -s \left(c_i^j + \frac{q_{i-1/2}^j}{2} \right), \\ \left(\frac{\partial F_{A,i}^j}{\partial A_{i+1}^j} \right) &= s \left(-c_{i+1}^j + \frac{q_{i+1/2}^j}{2} \right), \\ \left(\frac{\partial F_{A,i}^j}{\partial A_i^j} \right) &= s \left(c_i^j + c_{i+1}^j + \frac{q_{i+1/2}^j - q_{i-1/2}^j}{2} + \phi_i^j \phi_{w,i}^j (1 + r m_A B_i^j) \right). \end{aligned}$$

Here we let $F_{A,i}$ denote the equation of A_i similar to F_i in section 3.4. We get similar derivatives for the equations for B . The linearized systems will be coupled together similar to the linear systems in section 3.5.

In the end we find C^j using ϕ^j, p^j, A^j and B^j . We will solve implicitly for C too. The precipitation term f_{Prec} is a linear function of C , $f_{\text{Prec}} = S_{\text{Prec}} C - S_{\text{Prec}} C_{\text{eq}}$. Thus we have a linear equation for C , which can be solved using a discretization scheme similar to eq. (3.43) in section 3.3.

Chapter 4

Numerical results

This chapter gives the numerical results of the simulations using the discretization described in the previous chapter. We first did a convergence test with a constructed analytical solution, to check the method's converge, before we used the method on an example of modeling of concrete carbonation.

4.1 Comparison with analytical solution

The purpose of this section is to show that the numerical solution of the system converges. We will do it in the same way as they did in the article of Radu et al. [39], by constructing an analytical solution to fit the system, and do several numerical simulations with different sizes of the time and space steps. Further, we will compare the numerical solutions we get, with the constructed analytical solutions by computing the errors. What we mean by a constructed numerical solution, is that we choose a simple solution we know satisfies the given boundary and initial conditions, and we adjust the equations such that the analytical solutions will be the exact solutions of the set of equations.

4.1.1 The set of equations

In this comparison test, we will make some simplifications to the equations eqs. (3.48) to (3.55). First, we will also assume that the porosity is constant by taking $S_{\text{Diss}} = S_{\text{Prec}} = 0$. That is, presuming there is no dissolution of $\text{Ca}(\text{OH})_2$ or precipitation of CaCO_3 . Then eq. (3.53) decouples from the rest of the equations and gives $\phi = \phi_I$, the initial value of the porosity. Because the porosity then is constant, we can divide through the equations by it, and the ϕ disappears from the eqs. (3.48) to (3.52), and we get a simplified set

of equations. To simplify the equations even more, we let both the density ρ and the parameter in the reaction-term r , be equal to identity

$$\rho = r = 1,$$

as well as the diffusion coefficients D_A , D_B and D_C , that is

$$D_A = D_B = D_C = 1.$$

Doing these simplifications and adding functions to the right hand side of the equations, eqs. (3.48) to (3.52) gives us the following set of equations

$$(\phi_w)_t + v_x = \phi_w AB + f(x, t), \quad (4.1)$$

$$v = -K_S k p_x, \quad (4.2)$$

$$(\phi_w A)_t + (-D_A \phi_w A_x + vA)_x = -\phi_w m_A AB + f_A(x, t), \quad (4.3)$$

$$(\phi_w B)_t + (-D_B \phi_w B_x + vB)_x = -\phi_w m_B AB + f_B(x, t), \quad (4.4)$$

$$(\phi_w C)_t + (-D_C \phi_w C_x + vC)_x = \phi_w m_C AB + f_C(x, t), \quad (4.5)$$

which are the set of equations we will solve numerically in the domain $0 \leq x \leq 1$ for $0 \leq t \leq 1$. In these equations, we choose the absolute permeability $K_S = 2$, and the molecular weights of the species are given from [39] as

$$m_A = 44,$$

$$m_B = 74,$$

$$m_C = 100.87.$$

We will also use the same expressions for the water saturation ϕ_w and the relative permeability $k(\phi_w)$ as they did in Radu et al. [39] for their comparison with constructed analytical solutions. They are both given as functions for the pressure p , given as

$$\phi_w(p) = \frac{1}{1-p}, \quad (4.6)$$

$$k(p) = p^2. \quad (4.7)$$

In addition to eqs. (4.1) to (4.7), we need initial and boundary conditions for A, B, C and p . We choose the initial conditions

$$p(x, 0) = -1,$$

$$A(x, 0) = B(x, 0) = C(x, 0) = 1,$$

for $0 < x < 1$, and Dirichlet boundary conditions

$$\begin{aligned} p(0, t) &= p(1, t) = -1, \\ A(0, t) &= B(0, t) = C(0, t) = 1, \\ A(1, t) &= B(1, t) = C(1, t) = 1, \end{aligned}$$

for $t \geq 1$. We then construct analytical solutions for A, B, C and p . The following solutions will satisfy the given initial and boundary conditions for $x \in [0, 1]$,

$$\hat{p}(x, t) = -1 - tx(1 - x), \quad (4.8)$$

$$\hat{A}(x, t) = 1 + tx(1 - x). \quad (4.9)$$

and

$$\hat{C}(x, t) = \hat{B}(x, t) = \hat{A}(x, t). \quad (4.10)$$

We will now find the functions we will add on the right hand side of the equations. Inserting the analytical solutions $\hat{p}, \hat{A}, \hat{B}$ and \hat{C} into eqs. (4.1) and (4.3) to (4.5) will provide us with expressions for f, f_A, f_B and f_C . From eqs. (4.1) and (4.2), we see

$$f(x, t) = (\phi_w(\hat{p}))_t - K_S (k_x(\hat{p})\hat{p}_x + k(\hat{p})\hat{p}_{xx}) - \phi_w(\hat{p})\hat{A}\hat{B}.$$

And when we set in for k and the partial derivatives of ϕ_w and k with respect to t and x respectively, we get

$$f(x, t) = \frac{1}{(1 - \hat{p})^2} \hat{p}_t - K_S (2\hat{p}(\hat{p}_x)^2 + \hat{p}^2 \hat{p}_{xx}) - \frac{\hat{A}\hat{B}}{1 - \hat{p}}, \quad (4.11)$$

where the considered partial derivatives of \hat{p} are

$$\begin{aligned} \hat{p}_t &= -x(1 - x), \\ \hat{p}_x &= -t(1 - 2x), \\ \hat{p}_{xx} &= 2t. \end{aligned}$$

Equation (4.11) gives us an expression for f . We want to find corresponding expression for f_A, f_B and f_C . Equation (4.3) gives

$$f_A(x, t) = \left(\phi_w(\hat{p})\hat{A} \right)_t + \left(-\phi_w(\hat{p})\hat{A}_x + \hat{v}\hat{A} \right)_x + \phi_w(\hat{p})m_A\hat{A}\hat{B}.$$

where $\hat{v} = -K_S k(\hat{p})\hat{p}_x$. Applying the product rule for derivatives to the above formula for f_A , leads to the following expression

$$f_A = \frac{\partial \hat{\phi}_w}{\partial t} \hat{\phi}_w \hat{A} + \hat{\phi}_w \hat{A}_t - \frac{\partial \hat{\phi}_w}{\partial x} \hat{A}_x - \hat{\phi}_w \hat{A}_{xx} + \hat{v}_x \hat{A} + \hat{v} \hat{A}_x + \hat{\phi}_w m_A \hat{A} \hat{B}.$$

We replace ϕ_w and the partial derivatives of ϕ_w with respect x and t , with their formulas in terms of \hat{p} , collect terms, and get

$$f_A(x, t) = \frac{\hat{p}_t \hat{A} - \hat{p}_x \hat{A}_x}{(1 - \hat{p})^2} + \frac{\hat{A}_t - \hat{A}_{xx} + m_A \hat{A} \hat{B}}{1 - \hat{p}} + \hat{v}_x \hat{A} + \hat{v} \hat{A}_x. \quad (4.12)$$

The derivative of \hat{v} with respect to x is

$$\hat{v}_x = -K_S (2\hat{p}(\hat{p}_x)^2 + k(\hat{p})\hat{p}_{xx}),$$

and the partial derivatives of \hat{A} are found from eq. (4.9) as

$$\begin{aligned} \hat{A}_t &= x(1 - x), \\ \hat{A}_x &= t(1 - 2x), \\ \hat{A}_{xx} &= -2t. \end{aligned}$$

We get expressions similar to eq. (4.12) for f_B and f_C ,

$$f_B(x, t) = \frac{\hat{p}_t \hat{B} - \hat{p}_x \hat{B}_x}{(1 - \hat{p})^2} + \frac{\hat{B}_t - \hat{B}_{xx} + m_B \hat{A} \hat{B}}{1 - \hat{p}} + \hat{v}_x \hat{B} + \hat{v} \hat{B}_x, \quad (4.13)$$

$$f_C(x, t) = \frac{\hat{p}_t \hat{C} - \hat{p}_x \hat{C}_x}{(1 - \hat{p})^2} + \frac{\hat{C}_t - \hat{C}_{xx} - m_C \hat{A} \hat{B}}{1 - \hat{p}} + \hat{v}_x \hat{C} + \hat{v} \hat{C}_x. \quad (4.14)$$

\hat{B} and \hat{C} are equal to \hat{A} , thus their derivatives will also be equal to the derivatives of \hat{A} .

When inserting the functions f, f_A, f_B and f_C , eqs. (4.11) to (4.14) into eqs. (4.1) and (4.3) to (4.5), we get the equations we want to solve.

4.1.2 Comparison results

Now, we have got a set of equations to solve, whose numerical solutions, we can compare with the analytical ones, eqs. (4.8) to (4.10). We will solve them numerically as shown in chapter 3. In section 3.6 we describe how each of them are solved. Here we have constant Dirichlet boundary conditions for the A, B and C , and they are treated as the boundary conditions for p in section 3.2.3.

To compare the numerical solution with the analytical one, we need some measure for the difference between them, in form of a norm. We will use the L^2 -norm, which is given as

$$\|u\|_2 = \left(\int |u|^2 \right)^{1/2},$$

for a function u [10]. We will compute the error for p and each of the species A, B and C as

$$\mathbf{E} = \|u_{anal}(x, T) - u_{num}(x, T)\|_2, \quad (4.15)$$

where $u_{anal}(x, T)$ and $u_{num}(x, T)$ are the analytical and numerical solution respectively at $t = T$, the end time. In this test, we let $t \in [0, 1]$, thus $T = 1$. Then the squared error is given by

$$\mathbf{E}^2 = \|u_{anal}(x, T) - u_{num}(x, T)\|_2^2 = \int_0^1 |u_{anal}(x, T) - u_{num}(x, T)|^2 dx,$$

for $x \in [0, 1]$. Recall, when we solve the equations numerically, we divide the interval $[0, 1]$ into subintervals we call cells with the midpoints x_1, x_2, \dots, x_n , and integrate over each cell, see chapter 3. We do the same here, and get

$$\mathbf{E}^2 = \sum_{i=1}^n \int_{x_{i-1/2}}^{x_{i+1/2}} |u_{anal}(x, T) - u_{num}(x, T)|^2 dx,$$

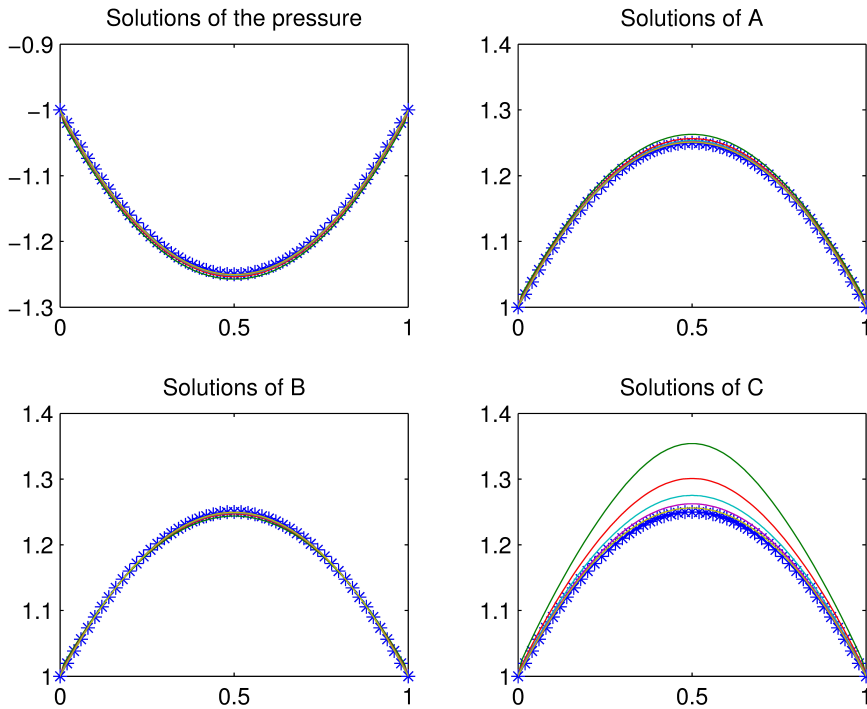


Figure 4.1: Numerical solutions for $h = \tau = 0.02, 0.01, 0.005, 0.0025, 0.00125$ compared to the analytical solutions marked with by stars.

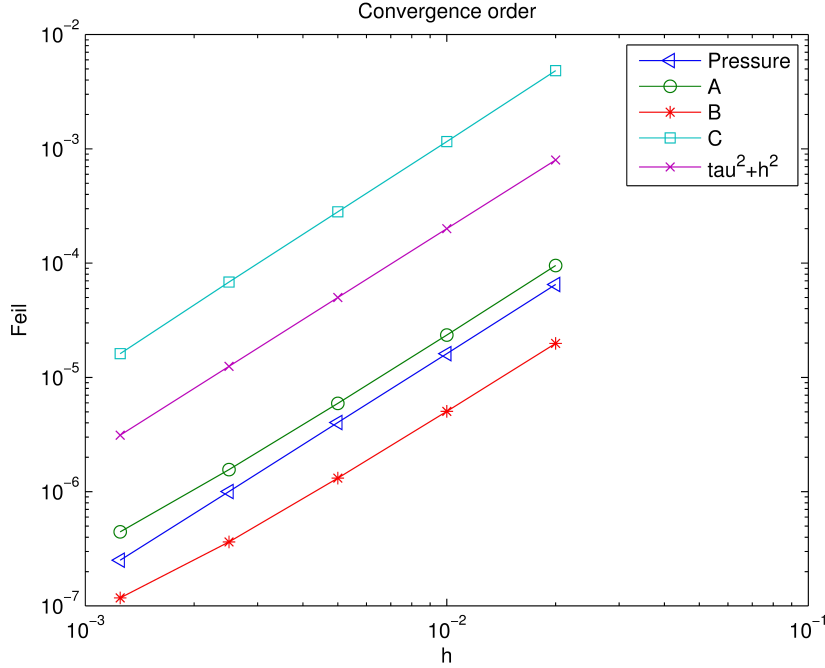


Figure 4.2: Convergence for $h = \tau$ from $h = 0.02$.

which becomes

$$\mathbf{E}^2 = \sum_{i=1}^n h |u_{anal,i}^T - u_{num,i}^T|^2, \quad (4.16)$$

when we approximate the integrals over each of the subintervals $[x_{i-1/2}, x_{i+1/2}]$ by the midpoint rule. h is the length of the interval.

We perform the convergence test by running the code for $\tau = h$ from $h = 0.02$, halving the step sizes for each time. Figure 4.1 show the solutions for step size $h = 0.02, 0.01, 0.005, 0.0025, 0.00125$. The numerical solutions for the pressure p and the species A, B and C compared to the analytical solutions eqs. (4.8) to (4.10) marked with blue stars. The numerical solutions converges to the analytical ones, getting closer and closer to them for smaller step sizes. When we compute the squared errors, eq. (4.16), we see that the numerical solutions converges by $O(\tau^2 + h^2)$ to the analytical solutions. Figure 4.2 that the squared errors are proportional to $\tau^2 + h^2$. This conforms the first order convergence of the method, and its as good at the one used in Radu et al. [39]. They used finite element method.

4.2 Numerical simulations

When we now have established the convergence of the method, we can use it to do some numerical simulations for the concrete carbonation problem. We will start by using the same parameters as they did in Radu et al. for the concrete carbonation problem. We consider again eqs. (3.48) to (3.53) in section 3.6. We repeat them here,

$$\begin{aligned}
(\phi\phi_w)_t + q_x &= \frac{\phi\phi_w}{\rho}rAB, \\
q &= -K_S\phi k(\phi_w)p_x, \\
(\phi\phi_w A)_t + (-D_A\phi\phi_w A_x + qA)_x &= -r\phi\phi_w m_A AB, \\
(\phi\phi_w B)_t + (-D_B\phi\phi_w B_x + qB)_x &= f_{\text{Diss}}\phi\phi_w - r\phi\phi_w m_B AB, \\
(\phi\phi_w C)_t + (-D_C\phi\phi_w C_x + qC)_x &= -f_{\text{Prec}}\phi\phi_w + r\phi\phi_w m_C AB, \\
\phi_t &= s(\phi - \delta)\frac{1 - \phi}{Z_\phi + (1 - \phi)}(\phi_w f_{\text{Diss}} - \phi_w f_{\text{Prec}}).
\end{aligned}$$

In addition we assume the constitutive relations for the water saturation ϕ_w and relative permeability k has the form

$$\begin{aligned}
\phi_w(p) &= \phi_{w,max}(1 + (-\alpha p)^n)^{-m}, \\
k(\phi_w) &= \sqrt{\phi_w}(1 - (1 - \phi_w^{1/m})^m)^2,
\end{aligned}$$

given by van Genuchten-Mualem parametrization. See section 2.3.

Note, in their case, they look at a 2-d problem, in the plane, where their y -direction is our x -direction. We will keep the x -indices in our equations. They also assume the model is dimensionless [39].

We will use Newton method again to solve for the pressure p , and we need then the derivative of ϕ_w with respect to p . It is found to be

$$\frac{d\phi_w}{dp} = \alpha(n - 1)\phi_{w,max}(1 + (-\alpha p)^n)^{-m-1}(-\alpha p)^{n-1}.$$

We consider the space domain $x \in [0, 1]$. On this interval, we define the initial conditions, and the boundary conditions are give at $x = 0$ and $x = 1$. As in [39], we give the initial condition of the pressure p as

$$p(x, 0) = 0.001(x - 2),$$

and having the Dirichlet boundary conditions

$$\begin{aligned}
p(0, t) &= -0.002, \\
p(1, t) &= -0.001.
\end{aligned}$$

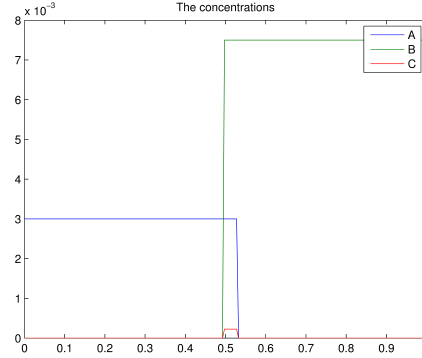


Figure 4.3: Initial values for A , B and C for $r = 10$.

We further assume as in [39], there is at $t = 0$ some amount of CO_2 and $\text{Ca}(\text{OH})_2$, but no CaCO_3 . The initial conditions are then defined as

$$A(x, 0) = \begin{cases} 3 \cdot 10^{-3}, & \text{for } 0 \leq x \leq 0.53, \\ 0, & \text{for } 0.53 < x \leq 1, \end{cases}$$

for the concentration of CO_2 ,

$$B(x, 0) = \begin{cases} 0, & \text{for } 0 \leq x < 0.5, \\ 0.0075, & \text{for } 0.5 \leq x \leq 1, \end{cases}$$

give the initial concentration of $\text{Ca}(\text{OH})_2$, and the initial concentration of CaCO_3 is

$$C(x, 0) = rA(x, 0)B(x, 0), \quad \text{for } 0 \leq x \leq 1.$$

Figure 4.3 shows the initial concentrations of CO_2 , $\text{Ca}(\text{OH})_2$ and CaCO_3 for $r = 10$, and fig. 4.4 shows the initial concentrations for $r = 1000$. The initial conditions are chosen in such a way that we assume the species A and B has already started to react with each other.

We assume we have homogeneous Neumann boundary conditions for A , B and C ,

$$\begin{aligned} A_x(0, t) &= A_x(1, t) = 0, \\ B_x(0, t) &= B_x(1, t) = 0, \\ C_x(0, t) &= C_x(1, t) = 0. \end{aligned}$$

The model parameters further are the same as in [39], where they choose the water density $\rho = 1$ and the absolute permeability $K_S = 2.0$. Further, $\alpha = 0.152$, $n = 4.0$ and the maximal water saturation $\phi_{w,max} = 0.5$. For the

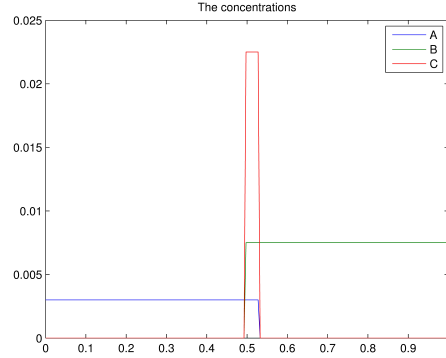


Figure 4.4: Initial values for A , B and C for $r = 1000$.

dissolution and precipitation rates, $S_{\text{Diss}} = 0.0067$, $B_{\text{eq}} = 0.0075$, S_{Prec} and C_{eq} . Choosing these values, we assume there is dissolution of $\text{Ca}(\text{OH})_2$, but no precipitation of CaCO_3 . The values of the regularization parameters are $\delta = 0.001$ and $Z_\phi = 0.01$. And the diffusion coefficients are taken as

$$\begin{aligned} D_A &= 1.0, \\ D_B &= 0.0864, \\ D_C &= 0.000864, \end{aligned}$$

where as the molecular weight are

$$\begin{aligned} m_A &= 44, \\ m_B &= 74, \\ m_C &= 100.87. \end{aligned}$$

With these parameters and conditions, we run simulations with step size $h = 0.005$ for $r = 10$ and $r = 1000$. The numerical solutions for A , B and C are shown in figs. 4.5 and 4.6 for $r = 10$ and $r = 1000$, respectively. The solutions are shown in both cases for $t = 0.1$ and $t = 1$, and we see how the concentrations change. As time goes by, the concentrations of CO_2 and $\text{Ca}(\text{OH})_2$ go down as they are consumed in the reaction, while the CaCO_3 is produced in the reaction, and its concentration increases. When $r = 1000$, the reaction is much faster than when $r = 10$, and the amount of CaCO_3 grows faster without spreading so much out. Our concentration profiles have the same tendencies as the concentration profiles in Radu et al. [39], but our values are a bit higher. We do not have quite the same initial conditions as in their simulations whose results is shown in [39]. This might have an effect. We see from the initial condition figs. 4.3 and 4.4 a great effect of the value

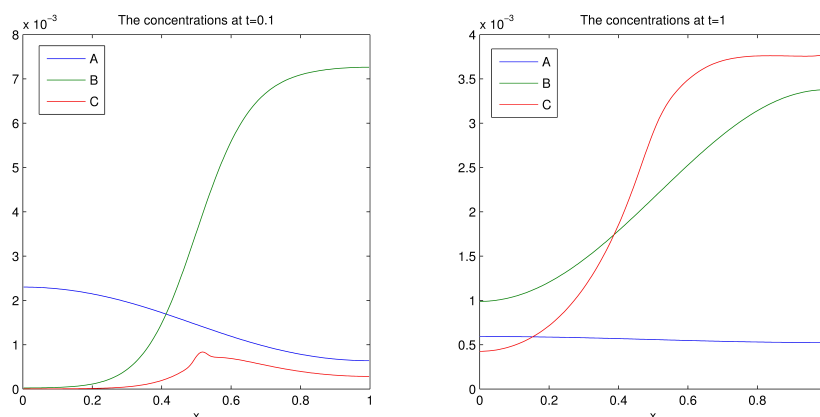


Figure 4.5: The concentrations of CO_2 , $\text{Ca}(\text{OH})_2$ and CaCO_3 at time $t = 0.1$ and $t = 1$ when $r = 10$ and $h = 0.005$.

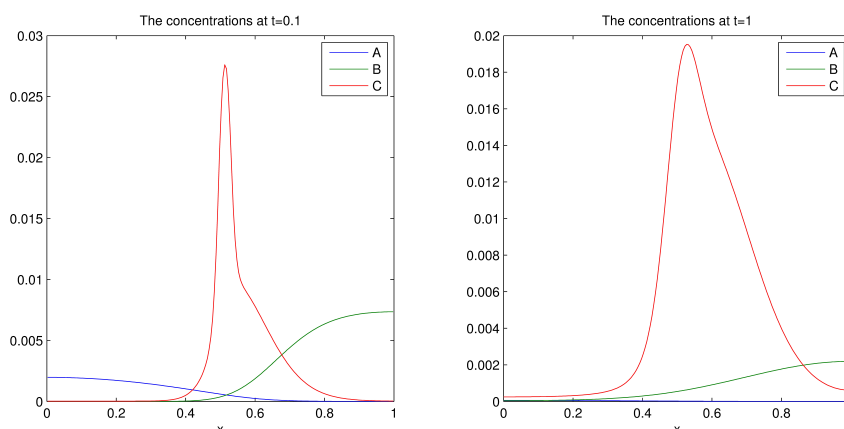


Figure 4.6: The concentrations of CO_2 , $\text{Ca}(\text{OH})_2$ and CaCO_3 at time $t = 0.1$ and $t = 1$ when $r = 1000$ and $h = 0.005$.

of r on the initial condition, and we see how these initial conditions effects the solutions at later times in figs. 4.5 and 4.6, in the way that the initial conditions determines the shapes of the concentration profiles at later times.

When we have homogeneous Neumann boundary conditions, we assume that there is no flow across the boundary. This means, we do not get any supply of CO_2 or $\text{Ca}(\text{OH})_2$. We will now consider the boundary and initial conditions they apply in the article of Papadakis et al. [32]. They assume we have a concrete sample, where $x = 0$ denotes the edge of the concrete exposed to CO_2 from the outside. Therefore, on this boundary, they take constant Dirichlet boundary conditions for CO_2 , giving a constant input of carbon

dioxide. Further, we assume that initially, there is no CO_2 in the concrete sample. If $t = 0$ is the end of the curing period, that is when the sample no longer is completely filled with water, and carbon dioxide can start to diffuse in through the concrete. We then also can assume a constant value for the concentration of $\text{Ca}(\text{OH})_2$, when it has not yet reacted to CO_2 . Summing up, the initial conditions are then

$$\begin{aligned} A(x, 0) &= 0, \\ B(x, 0) &= B_I, \\ C(x, 0) &= 0, \end{aligned}$$

for $0 \leq x \leq 1$. Boundary conditions for A are given as

$$A(0, t) = A_O, \quad A_x(1, t) = 0,$$

and for the rest, we have homogeneous Neumann boundary conditions

$$\begin{aligned} B_x(0, t) &= B_x(1, t) = 0, \\ C_x(0, t) &= C_x(1, t) = 0. \end{aligned}$$

We do the simulations for $h = 0.005$, $\tau = 0.02$ and $r = 1000$, and plot the

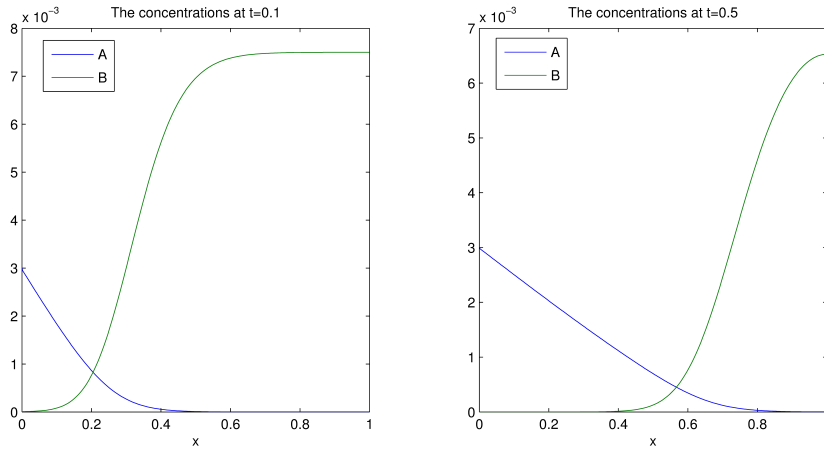


Figure 4.7: The concentrations of CO_2 and $\text{Ca}(\text{OH})_2$ at time $t = 0.1$ and $t = 0.5$, for $r = 1000$ and Dirichlet boundary condition for A at $x = 0$.

results at $t = 0.1$ and $t = 0.5$. The solutions for A and B are shown in fig. 4.7. We see that we in this case, have similar concentration profiles as the ones in the articles of Meier et al. [27] and Peter et al. [36], where we see how the reaction front moves towards the boundary $x = 1$. From the figure,

we also see how we have a constant source of CO_2 at the boundary $x = 0$, as $\text{Ca}(\text{OH})_2$ is bounded by the carbon dioxide.

Here we let $A_O = 3 \cdot 10^{-3}$ and $B_I = 0.0075$, corresponding to the initial conditions in the previous example. We do this here, even though it is naturally to assume that the initial concentration of B is higher here than in the previous case, as well to assume the A_O is higher than the initial value of A in the previous case. Because in that case, the species already had started to react with each other, while in this case, we assume the initial state is right before they start to react with each other. But we do not have any other values for A_O and B_I now.

Where the graphs of A and B in fig. 4.7 intersects, we find the reaction layer, and we can see how it moves. When we compare to the results for the same case when $r = 10$ fig. 4.8, we see we do not get this sharp reaction front there.

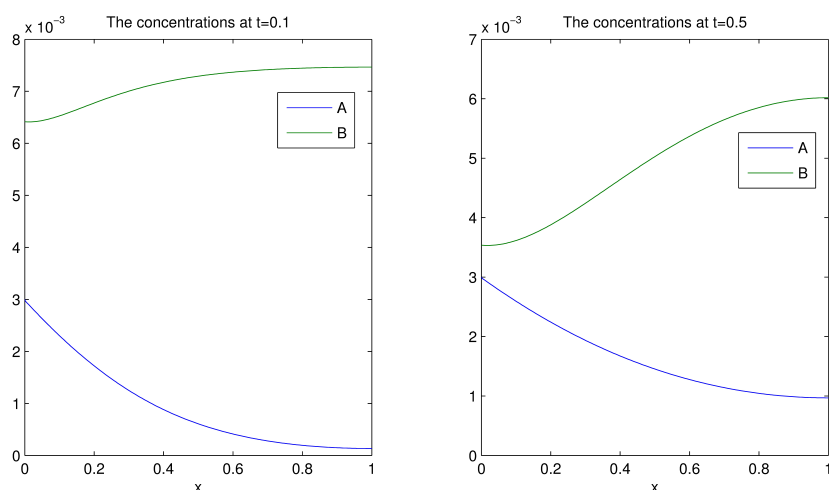


Figure 4.8: The concentrations of CO_2 and $\text{Ca}(\text{OH})_2$ at time $t = 0.1$ and $t=0.5$, for $r = 1000$ and Dirichlet boundary condition for A at $x = 0$.

Chapter 5

Conclusion

We have performed several numerical simulations for our model of concrete carbonation, for the reaction rate constants $r = 10$ and $r = 1000$, seeing how the value of r effects the reaction. As expected, $r = 1000$ gives a much faster reaction than for $r = 10$. In the latter case, CO_2 and $\text{Ca}(\text{OH})_2$ spread more out on the domain through diffusion and flow, and we do not get this sharp reaction front characterizing concrete carbonation. Of course, the production of CaCO_3 is also slower for $r = 10$ than for $r = 1000$.

We could have used the parameters in Meier et al. [27] and get a better basis for comparing the results in fig. 4.7. Their boundary conditions are a bit different to the ones we assumed in this case, but we could have tried to get the same results. Our model is supposedly non-dimensional, but we have not given the units of the parameters involved or how the dimensional analysis should be done. In Meier et al. and Peter et al. they do dimensional analysis [27,36]. It had been interesting have comparable values of the reaction depth. Now the values for the reaction depth in our results, can not be compared to the ones in Meier et al. and Peter et al., we can only see that our profiles for $r = 1000$ at $t = 0.1$ and $t = 0.5$, has similar shape to the ones in [27, 36].

We have not investigated the influence of the concrete carbonation reaction on the porosity. Papadakis et al. [32] states there is a measurable decrease in porosity as a result of concrete carbonation. This decrease comes from the precipitation of CaCO_3 formed in the reaction, but we let $S_{\text{Diss}} = 0$ assuming no precipitation, that is way the concentration of CaCO_3 just grows and grows in figs. 4.5 and 4.6. If we plot porosity, we would have seen that it just increases, due to the precipitation of $\text{Ca}(\text{OH})_2$ and not decrease. We would have liked to have values for S_{Diss} and C_{eq} which would give us a decrease in porosity.

When it comes to the water flow and water saturation, we would have had more experimental data on how the water flow in the concrete, and

how to model it. If there is any flow to consider or not. Choosing the van Genuchten-Mulean parameterization here only gave us $\phi_w = \phi_{w,max}$ due to the little change in pressure. These equations are taken from reservoir modeling, where there are big pressure differences.

Bibliography

- [1] Reinforcement for Concrete-materials and Applications. <http://www.concrete.org/general/fE2-00.pdf>, 2000. ACI Education Bulletin E2-00, American Concrete Institute.
- [2] I. Aavatsmark. Bevarelsesmetoder for elliptiske differensialligninger. Lecture notes, University of Bergen, 2007.
- [3] I. Aavatsmark. Multipoint flux approximation methods for quadrilateral grids. Lecture notes, 9th International Forum on Reservoir Simulation, Abu Dhabi, 2007.
- [4] R. A. Adams. *Calculus: A Complete Course*. Pearson, 6th edition, 2006.
- [5] P. Atkins and J. de Paula. *Elements of Physical Chemistry*. Oxford University Press, 5th edition, 2009.
- [6] J. Brown. Concrete Carbonation - A Guide to the Different Types. <http://carboncure.com>, June 2012.
- [7] R. Cammack, T. Atwood, P. Campbell, H. Parish, A. Smith, F. Vella, and J. Stirling, editors. *Oxford Dictionary of Biochemistry and Molecular Biology*. Oxford University Press, 2nd edition, 2006.
- [8] R. Chang and J. Overby. *General Chemistry: The Essential Concepts*. McGraw-Hill, sixth edition, 2011.
- [9] Z. Chen, G. Huan, and Y. Ma. *Computational Methods for Multiphase Flows in Porous Media*. SIAM, 2006.
- [10] W. Cheney. *Analysis for Applied Mathematics*. Springer, 2001.
- [11] J. M. Cooper. *Introduction to Partial Differential Equations with MATLAB*. Birkhäuser, 1998.

-
- [12] J. S. Curl. *A Dictionary of Architecture and Landscape Architecture*. Oxford University Press, 2nd edition, 2006.
- [13] J. Daintith, editor. *A Dictionary of Chemistry*. Oxford University Press, 6th edition, 2008.
- [14] I. Danaila, P. Joly, S. M. Kaber, and M. Postel. *An Introduction to Scientific Computing, Twelve Computational Projects Solved with MATLAB*. Springer, 2007.
- [15] A. Dokoumetzidisa and P. Macheras. A century of dissolution research: From Noyes and Whitney to the Biopharmaceutics Classification System. *International Journal of Pharmaceutic*, 321:1–11, 2006.
- [16] L. C. Evans. *Partial Differential Equations*, volume 19 of *Graduate Studies in Mathematics*. American Mathematical Society, 2002.
- [17] G. F. Froment, K. B. Bischoff, and J. De Wilde. *Chemical Reactor: Analysis and Design*. John Wiley & Sons, 3rd edition, 2011.
- [18] C. F. Gerald and P. O. Wheatley. *Applied Numerical Analysis*. Pearson, 7th edition, 2004.
- [19] T. C. Holland. Silica Fume User’s Manual. <http://www.silicafume.org/concrete-manual.html>, April 2005. Silica Fume Association.
- [20] H. Honour and J. Fleming. *A World History of Art*. Laurence King, 5th edition, 1999.
- [21] J. Hu. *Porosity of Concrete: Morphological Study of Model Concrete*. PhD thesis, Delft University of Technology, 2004.
- [22] D. Kincaid and W. Cheney. *Numerical Analysis: Mathematics of Scientific Computing*. Brooks/Cole, 3th edition, 2002.
- [23] F. Kind-Barkauskas, B. Kauhsen, S. Polónyi, and J. Brandt. *Concrete Construction Manual*. Birkhäuser, 2002.
- [24] P. Knabner and L. Angemann. *Numerical Methods for Elliptic and Parabolic Partial Differential Equations*. Springer, 2003.
- [25] S. Kostof. *A History of Architecture: Settings and Rituals*. Oxford University Press, 2nd edition, 1995.
- [26] W. K. Lewis and W. G. Whitman. Principles of Gas Absorption. *Industrial and Engineering Chemistry*, 16:1215–1220, 1924.

- [27] S. A. Meier, M. A. Peter, A. Muntean, and M. Böhm. Dynamics of the internal reaction layer arising during carbonation of concrete. *Chemical Engineering Science*, 62:1125–1137, 2007.
- [28] A. Muntean and M. Böhm. A moving-boundary problem for concrete carbonation: Global existence and uniqueness of weak solutions. *Journal of Mathematical Analysis and Applications*, 350:234–251, 2009.
- [29] A. Muntean, M. Böhm, and J. Kropp. Moving carbonation fronts in concrete: A moving-sharp-interface approach. *Chemical Engineering Science*, 66:538–547, 2011.
- [30] J. Newman and B. S. Choo, editors. *Advanced Concrete Technology 2: Concrete Properties*. Butterworth-Heinemann, 2003.
- [31] J. M. Nordbotten and M. A. Celia. *Geological Storage of CO₂, Modeling Approaches for Large-Scale Simulation*. Wiley, 2012.
- [32] V. G. Papadakis, C. G. Vayenas, and M. N. Fardis. A reaction engineering approach to the problem of concrete carbonation. *A.I.Ch.E. Journal*, 35:1639–1650, 1989.
- [33] V. G. Papadakis, C. G. Vayenas, and M. N. Fardis. Experimental investigation and mathematical modeling of the concrete carbonation problem. *Chemical Engineering Science*, 46:1333–1338, 1991.
- [34] Ch. Park. *A Dictionary of Environment and Conservation*. Oxford University Press, 2007.
- [35] M. Peck, editor. *Concrete: Design, Construction, Examples*. Birkhäuser Verlag AG, 2006.
- [36] M. A. Peter, A. Muntean, S. A. Meier, and M. Böhm. Competition of several carbonation reactions in concrete: A parametric study. *Cement and Concrete Research*, 38:1385–1393, 2008.
- [37] Ø. Pettersen. *Grunnkurs i reservoarmekanikk*. Matematisk institutt, Universitetet i Bergen, 1990.
- [38] A. Quarteroni, R. Sacco, and F. Saleri. *Numerical Mathematics*. Springer, 2007.
- [39] F. A. Radu, A. Muntean, I. S. Pop, N. Suciuciu, and O. Kolditz. A mixed finite element discretization scheme for a concrete carbonation model with concentration-dependent porosity. *Journal of Computational and Applied Mathematics*, 246:74–85, 2013.

- [40] P. A. Ramachandran and M. M. Sharma. Absorption with fast reaction in a slurry containing sparingly soluble fine particles. *Chemical Engineering Science*, 24:1681–1986, 1969.
- [41] A. V. Sietta, A. Schrefler, and R. V. Vitaliani. The carbonation of concrete and the mechanism of moisture, heat and carbon dioxide flow through porous materials. *Cement and Concrete Research*, 23:761–772, 1993.
- [42] A. J. Salber and C. W. Swan. Design of fly-ash concrete masonry for optimal carbon sequestration. <http://www.flyash.info/2013/099-Salber-2013.pdf>, April 2013.
- [43] T. Siemes, R. Polder, and H. de Vries. Design of concrete structures for durability - Example: Chloride penetration in the lining of a bored tunnel. *HERON*, 43:227–244, 1998.
- [44] A. Steffens. *Modellierung von Karbonatisierung und Chloridbindung zur numerischen Analyse der Korrosionsgefährdung der Betongbewehrung*. PhD thesis, Institute for Structural Analysis, Technische Universität Braunschweig, 2000.
- [45] A. Steffens, D. Dinkler, and H. Ahrens. Modeling carbonation for corrosion risk prediction of concrete structures. *Cement and Concrete Research*, 32:935–941, 2002.
- [46] J. W. Thomas. *Numerical Partial Differential Equations: Finite Difference Methods*. Springer, 1995.
- [47] M. D. A. Thomas and J. D. Matthews. Carbonation of fly ash concrete. *Magazine of Concrete Research*, 44:217–228, 1992.
- [48] M. Th. van Genuchten. A Closed-form Equation for Predicting the Hydraulic Conductivity of Unsaturated Soils. *Soil Sci. Soc. Am. J.*, 44:892–898, 1980.
- [49] G. Villain, M. Thiery, and G. Platret. Measurement methods of carbonation profiles in concrete: Thermogravimetry, chemical analysis and gammadensimetry. *Cement and Concrete Research*, 37:1182–1192, 2007.